An Information-Decision Framework for the Multilevel Co-Design of Products, Materials, and Manufacturing Processes

Mathew Baby
Ph.D. Candidate
Department of Mechanical and Civil Engineering
Florida Institute of Technology, Melbourne, FL 32901, USA
mbaby2021@my.fit.edu

Anand Balu Nellippallil [1]
Assistant Professor
Department of Mechanical and Civil Engineering
Florida Institute of Technology, Melbourne, FL 32901, USA
anellippallil@fit.edu

ABSTRACT

Realizing products that meet targeted performance requires careful consideration of the material processing to identify appropriate material microstructures and associated mechanical properties. The integrated design of such systems involving products, materials, and manufacturing processes necessitates facilitating co-design - a collective and coordinated effort by the product, materials, and process designers at multilevel to share their resources, information, and knowledge for making effective design decisions using the Processing-microStructure-Property-Performance (PSPP) relations. Goal-oriented Inverse Design (GoID) is one approach to co-designing these systems. In GoID, multilevel decisions are targeted at meeting the goals propagated inversely from the top level in the design hierarchy. Nevertheless, achieving the inversely propagated goals from one level may not be feasible at another level owing to the goal targets, established constraints, and available bounds. This results in design conflicts between multilevel decisions, leading to a loss in multilevel and system performance.

In this paper, we propose an information-decision framework to model goal-directed, multilevel decision-making and interactions for products, materials, and manufacturing processes, detect potential conflicts between the multilevel decisions, and regulate the decisions to achieve improved multilevel and system performance. Decision regulation is achieved by studying the sensitivity of the goals to dominant design variables and constraints and making appropriate design modifications. We use a hot rod rolling problem to showcase the efficacy of the proposed framework in systematically detecting and managing conflicts while co-designing the product, material, and manufacturing processes involved. The framework is generic and facilitates the top-down co-design of multilevel systems involving products, materials, and manufacturing processes.

Keywords: Information-decision framework, Co-design, Multilevel design, Processing-microstructure-property-performance linkages, Inverse design, Decision-based design

1. FRAME OF REFERENCE

Manufacturers must produce products with targeted performance to meet the market requirements. Targeted product performance is achieved by ensuring an appropriate range of mechanical properties and material microstructures, which sometimes require the use of multi-material components [1-3]. The material processing during manufacturing influences the material microstructure, thus defining the mechanical properties and product performance. This interconnect among processing, microstructure, properties, and performance is illustrated using the hot rod rolling (HRR) process chain example. In HRR, cast steel billets are reheated and further processed in rolling and cooling mills to produce hot-rolled steel rods as products. The mechanical properties that identify the steel rod performance [4] are determined by the steel microstructure produced as a result of the above thermo-mechanical processing. Hence, the prudent management of the manufacturing processes involved in realizing the product is required to tailor the material microstructure and attain a specific range of mechanical properties, thereby satisfying the targeted product performance [5]. Given the inherent relationships between material processing, microstructure, achieved

[1] Corresponding author, Email: anellippallil@fit.edu
A previous version of this paper was presented at the ASME IDETC 2022 Conference (Paper Number IDETC2022-90836), Recognized as a Paper of Distinction.

mechanical properties, and end product performance, realizing products that meet targeted performance requires an integrated consideration of the system constituted by the products, its materials, and associated manufacturing processes.

Material selection approaches [6-8] are traditionally employed to achieve targeted product performance. It involves choosing materials with suitable properties from a set of available materials. Classical material selection approaches do not facilitate tailoring the material microstructures to meet specific mechanical property requirements. Realization of products with specific microstructure and mechanical properties typically involves many plant trials and lab-scale experiments [9] that are expensive and time-consuming. The relatively cheaper and quicker alternative is to use simulation-supported approaches for the integrated design of systems involving products, materials, and manufacturing processes. Simulation-supported integrated design approaches focus on meeting multiple conflicting mechanical property requirements in a top-down, inverse manner by intentionally engineering the material microstructure and identifying the appropriate processing paths. Such a conscious effort to engineer materials that meet specific mechanical properties and microstructure requirements is the focus of 'materials design.' Direction for materials design is provided by the Integrated Computational Materials Engineering (ICME) program [10], where the Processing-microStructure-Property-Performance (PSPP) design hierarchy proposed by Olson [11] is exploited to realize the integrated, top-down design of products and materials with the support of simulations. Here, product performance requirements are inversely mapped onto material properties, followed by mapping the material properties onto materials structure to realize the top-down, inverse design of materials that satisfy product performance requirements. McDowell and Olson [12] propose a systems approach to materials design in line with ICME, where the PSPP relations are utilized to realize an inverse, multilevel design of products with a targeted performance range and the material structural hierarchy. McDowell [13] recommends that integrated, multilevel materials design approaches should facilitate an understanding of the sensitivity of the material properties to material microstructure and material microstructure to its processing. The sensitivity analysis helps designers i) identify key design variables with significant sensitivities across the material structure and design hierarchy and ii) perform solution space exploration to identify design solutions that meet a targeted range of performance [4].

The simulation-supported, integrated, multilevel materials design approaches require the collaborative effort of distributed domain experts for the different levels of the design process, such as product designers, materials designers, and process designers. The domain experts make decisions regarding the material choice for the product, the development of materials with improved performance, and the processing of materials to produce the product based on their domain expertise. Nellippallil and co-authors [4] present the design of such systems as a collaborative effort of a group of distributed experts, defined as 'co-design.' In this paper, we adopt this definition of co-design as the ability of a group of distributed domain experts that involves product, materials, and process designers to share their resources, information, and knowledge for the integrated design of the products, materials, and manufacturing processes. The primary role of domain experts in co-design is that of decision-makers or designers who make decisions regarding the design problem that requires their expertise, given the information available. Independent domain expert decisions at individual levels can cause unintended impacts on other levels [14] due to limitations in the other levels' available resources, resulting in design conflicts. The resource limitations at a level are defined using constraints, bounds, and goal targets. If left unresolved, design conflicts can result in poor performance at different levels that accumulate and lead to poor system performance, where products fail to meet targeted performance. *In this paper, we address the issue of managing design conflicts in the multilevel co-design of products, materials, and manufacturing processes from a systems-based inverse design viewpoint.*

Several works in the literature address multilevel material design and establish inverse PSPP linkages for design. Adams and co-authors [15] present a framework to support inverse materials and process design problems by employing spectral representation to establish invertible relationships between material processing, resultant material structure, and properties. Kalidindi and co-authors [16, 17] present the materials knowledge systems (MKS) approach, which supports inverse materials design problems by facilitating the bi-directional information flow between different length scales during the concurrent multiscale modeling and simulation of different materials phenomenon. Chen and co-authors [18] present an inverse materials design approach that combines generative inverse design networks, backpropagation, and an active learning strategy. Kumar and co-authors [19] propose an inverse design framework for realizing metamaterials with desired properties by identifying optimal topologies using deep neural networks. Qian and co-authors [20] present an inverse design method that employs artificial neural networks to design architectured composite materials. Kim and co-authors discuss the inverse design of porous Zeolite material

using artificial neural networks [21]. Tsai and coauthors [22] present an inverse model that uses an artificial neural network coupled with a genetic algorithm to realize optical lenses with form accuracy using injection molding. The above approaches are characterized by the need for considerable knowledge or data and a clear understanding of the different material phenomena, material hierarchy, and flow of information in the hierarchy. Hence, these approaches are unsuitable for early-stage design exploration, with limited data availability and a rudimentary understanding of the various phenomena and information flows.

Approaches such as the analytical target cascading (ATC) [23], collaborative optimization (CO) [24], and bilevel integrated system synthesis (BLISS) [25] are proposed by the multidisciplinary optimization (MDO) [26-29] community for optimizing multilevel systems. In general, the focus of MDO approaches is on identifying point solutions at each level using rigorous optimization techniques. They usually involve a substantial number of iterations within and between levels using optimization loops until convergence is achieved. This is particularly challenging in early-stage design exploration, where the focus is on quickly identifying satisfactory design regions instead of a single unique point solution [30]. Moreover, fundamental limitations exist in using MDO approaches in a materials design environment involving the product and the manufacturing processes. When considering product and manufacturing process aspects during materials design, it is sensible to distribute the design activities to (i) efficiently utilize the knowledge and expertise of the designers across various domains in the *synthesis* process and (ii) avoid formulating and solving system-level problems that are overly large and computationally burdensome. In a recent effort, Ituarte and co-authors [14] put forth a computer-aided expert system to explore the PSPP linkages and carry out trade-off exploration and optimization in digital manufacturing. This is realized by coupling product design, manufacturing processes, and materials systems using surrogate models and MDO. The work demonstrates exploring optimization solutions in multiple disciplines, specifically product, material, and manufacturing, ensuring overall system performance. However, the issue of design conflicts that can arise when there are many objectives at individual levels or disciplines, especially at the early stages of design, needs further attention.

The fundamental assumption in MDO is the identification and passing of single-point optimum solutions among designers and a central decision-maker. This assumption is challenged by approaches that seek to identify and share ranged sets of solutions with distributed designers across design levels [31, 32]. By identifying ranged sets of solutions, designers are free to choose a solution from the set based on their preference. Systematic top-down, system-based approaches that support early-stage materials design exploration are discussed limitedly in the literature. Choi and co-authors [33] present a multilevel, top-down design method that facilitates distributed design, the Inductive Design Exploration Method (IDEM). IDEM is suitable for hierarchical design problems and managing uncertainty propagation across levels in the early design stages. Kern and co-authors [34] present a generic Python implementation of the IDEM, named pyDEM, which employs an open-source Python tool. IDEM has certain noted limitations, such as flexibility in design, discretization errors, the increased computational expense for improved accuracy, and restrictions on the number of design variables that can be considered, as discussed in [35]. Nellippallil and co-authors propose the Goal-oriented Inverse Design (GoID) approach to address some of these limitations [35]. Wang and co-authors [36] present a template-based ontological method based on the GoID approach to support design space exploration. In GoID, decision-making is considered a sequential process, with decisions at different levels of the design process being made by domain experts. These decisions are directed towards the goal targets that are inversely propagated from the succeeding level in the sequence, starting with the system performance requirements. The sequential decision-making in GoID may result in conflicts among decisions across different levels, subsequently resulting in the inability to achieve the required material microstructures and mechanical properties and reduced product performance. Hence, there exists a need to manage the potential design conflicts that can arise when using the GoID approach in the multilevel co-design of systems involving products, materials, and manufacturing processes.

We consider design from a systems design standpoint as a simulation-supported, integrated, top-down, decision-based process to satisfy a targeted range of performance requirements. We follow the Decision-Based Design (DBD) paradigm [37] that considers design a decision-making process, where the designers make a series of decisions, some sequentially while others concurrently. Decision Support Problem (DSP) techniques are developed by Mistree and co-authors [37] to support decision-making in DBD. DSP techniques are anchored in the notion of bounded rationality proposed by Herbert A. Simon [38]. We view the design problem from the philosophy of a "satisficer" and seek a ranged set of satisficing solutions. A '*satisficing solution*' [39] satisfies the design requirements for the conflicting goals and showcases good enough performance given the available information and models used. The compromise Decision Support

Problem (cDSP) [40] is one well-established DSP construct in the literature that is useful in exploring satisficing design solution sets for design problems with multiple conflicting goals. Ming and co-authors [41] present a computational platform named Platform for Decision Support in the Design of Engineering Systems (PDSIDES), where DSPs are represented as computational decision templates to facilitate the storage and reuse of decision-related knowledge. In this paper, we use the cDSP construct and templates within PDSIDES to i) capture problem-specific information, ii) formulate multilevel design problems involving the product, material, and manufacturing process, and iii) explore ranged sets of design solutions for multiple conflicting goals across multilevel.

From a DBD perspective, we hypothesize that the issue of design conflicts can be addressed using a decision support framework that facilitates i) goal-directed decision-making across the different levels of the design process, ii) cooperative decision-making between the levels by managing the interactions, and iii) regulation of the design space and decision-making at different levels to attain improved performance. We define cooperation as a situation where i) the design conflicts among decisions at various levels are managed to ensure coordination (MDC - Manage Design Conflicts), and ii) decisions are made in a manner that facilitates the achievement of the goals at other levels (FG = Facilitate Goals) [42, 43]. The management of design conflicts by regulating decisions at different levels requires a clear understanding of the impact of the decision variables at a level on the corresponding goals. As discussed previously, simulation-supported integrated materials design approaches, including GoID, are well suited to support sensitivity analysis, which will aid designers in identifying key design variables across different levels. Identifying key variables will enable more effective conflict management in the proposed framework by allowing decision regulation with minimum changes to the variables. Minimum changes to variables correspond to a situation where the least amount of additional resources is utilized in managing the conflict, which is beneficial.

The outline of this paper is as follows. The description of the problem is presented in Section 2. In Section 3, we present an information-decision framework for the multilevel co-design of products, materials, and manufacturing processes. We also discuss using the PDSIDES platform to formulate and execute DSPs and explore the solution space across multiple design levels in Section 3. We showcase the framework's efficacy in supporting the management of design conflicts using the HRR test problem in Section 4. In the HRR test problem, we focus on the interactions between the levels of the design process that involve processing (manufacturing process), microstructure (material), and mechanical properties of the rod (product). We close the paper with our contributions and closing remarks in Section 5. We present the empirical models used in the test problem and the problem formulations in Appendix A.

2. PROBLEM DESCRIPTION – DESIGN CONFLICTS IN THE MULTILEVEL, TOP-DOWN CO-DESIGN OF PRODUCTS, MATERIALS, AND MANUFACTURING PROCESSES

Realizing products with targeted performance involves tailoring the properties and associated material microstructure to required ranges by carefully managing material processing. The inherent relationship among material processing, microstructure, mechanical properties, and product performance necessitates the multilevel co-design of the system involving products, their materials, and manufacturing processes to realize products with targeted performance. The multilevel co-design of such systems involves integrated decision-making across the PSPP design hierarchy. Integrated decision-making is realized through a collaborative effort of domain experts, such as process, materials, and product designers, who make decisions across different levels of decision-making based on their expertise.

In this paper, we consider the use of the GoID approach [35] for the multilevel co-design of products, materials, and manufacturing processes, as depicted in Figure 1. The sequential decision-making in GoID begins with identifying satisficing solutions for the DSP at Level 1- cDSP ‘1,’ as indicated by ‘Start’ in Figure 1. At Level 1, product performance requirements defined in terms of the multiple mechanical property goals are considered. cDSP ‘1’ is formulated to help the product designer determine satisficing solutions that fulfill product performance requirements propagated from the end product. Given the design variable bounds, the design space for cDSP ‘1’ is limited to a small region depicted by the grey area marked ‘X’ in cDSP ‘1.’ Additionally, requirements regarding acceptable mechanical property goal values are set as constraints that will result in different feasible design spaces for each mechanical property goal. The feasible design spaces corresponding to two mechanical property goals of cDSP ‘1’ are indicated by the red region marked ‘a’ and the blue region marked ‘b.’ In a situation with conflicting mechanical property goals, achieving all the goal targets might not be possible. The product designer seeks ‘satisficing solutions’ regarding material microstructure that fulfills the designer's requirements for the mechanical property goals and picks the green Region 1 in cDSP ‘1’. Hence, at Level 1, the designer considers the materials and product design aspects

together, with the material microstructure as inputs and mechanical properties of the product as outputs for cDSP '1'.

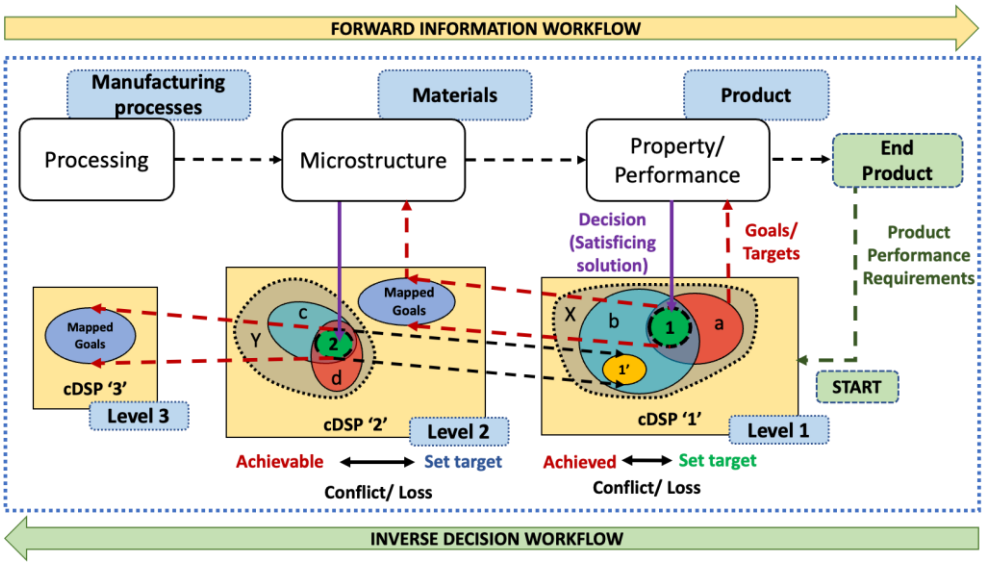

FIGURE 1: An illustration of the possible situation of conflict between multilevel decisions when using the GoID approach and subsequent loss in performance

The microstructure solutions identified are then propagated as goal targets for the DSP of the next level in the sequence - Level 2, as depicted by the blue 'Mapped Goals' region in cDSP '2.' At Level 2, the material requirements defined in terms of microstructure at the end of the final manufacturing process in the processing sequence are considered. The feasible design spaces corresponding to two microstructure goals of cDSP '2' are indicated by regions marked 'c' (blue) and 'd' (red) in the grey area marked 'Y.' The materials designer explores the feasible design spaces, seeking satisficing solutions in terms of processing variables that fulfill the designer's requirements for the potentially conflicting microstructure goals. The exploration ends with the materials designer picking the green Region 2 in cDSP '2'. Hence, at Level 2, the materials designer considers the materials and manufacturing processing aspects together, with processing variables as inputs and material microstructure as outputs for cDSP '2.' Since the microstructure goals are propagated to the cDSP '2' in a top-down manner, there is a lack of a way in GoID for the product and material designers at the interacting Levels 1 and 2 to collaborate and check if the microstructure goals mapped from Level 1 are achievable at Level 2, given the resources available. Design conflicts occur between the product and materials designers if the microstructure goal values corresponding to the satisficing solution picked at Level 2 do not meet the mapped microstructure goals from Level 1. The design conflicts arise primarily due to the limited resources defined in terms of constraints, bounds, and goals of conflicting nature in cDSP '2' that restrict the design space of the next level in the sequence, Level 2. The design conflicts lead to a loss in performance of both interacting levels, which is schematically represented in Figure 1. At Level 2, the achievable satisficing solution depicted by the green Region 2 does not match the targeted 'Mapped Goals' from Level 1, indicating a loss in performance at Level 2. The yellow Region 1' that depicts the goal values achieved at Level 1 by mapping back the satisficing solutions from Level 2 does not match the initially identified satisficing solutions at Level 1 indicated by the green Region 1, thus indicating a loss in performance at Level 1.

The inverse sequential propagation of decisions from one level to the next and subsequent decision-making is continued along the multilevel system until all remaining manufacturing processes that influence the material microstructure are considered, as depicted by Level 3 in Figure 1. With the solutions being propagated inversely, further conflicts may arise between multilevel decisions, resulting in performance losses and accumulation across the different levels, thus leading to poor system performance. Poor system performance will result in products failing to meet targeted performance. To address the above issue, top-down design approaches such as the GoID require a way to model the multilevel interactions and facilitate collaboration between the multilevel decisions. Facilitating the modeling of interactions will help the designers regulate the multilevel decisions to support cooperative decision-making, thereby ensuring multilevel and system performance in situations where design conflict exists. An information-decision framework to address the issue of design conflicts and ensure multilevel and system performance in the

multilevel, top-down co-design of products, materials, and manufacturing processes is presented in detail in the next section. We begin the next section by introducing the computational platform PDSIDES used to formulate the cDSPs, execute them, and explore satisficing solutions at different design levels.

3. INFORMATION-DECISION FRAMEWORK TO SUPPORT MULTILEVEL, TOP-DOWN CO-DESIGN OF PRODUCTS, MATERIALS, AND MANUFACTURING PROCESSES AND THE USE OF THE PDSIDES PLATFORM IN THE FRAMEWORK

In this section, we present an information-decision framework to facilitate cooperative decision-making and support multilevel, top-down co-design of products, materials, and manufacturing processes. Using the framework, we facilitate sequential, goal-directed decision-making across different levels and cooperative decision-making between the interacting levels by regulating design spaces and decisions at these levels. The regulation of decision-making at the interacting levels will aid design conflict management, thereby helping attain improved multilevel and system performance. We begin with Section 3.1, where we discuss the PDSIDES platform developed by Ming and co-authors [41] used to formulate and execute cDSPs and carry out solution space exploration in the framework.

3.1. Platform for Decision Support in the Design of Engineering Systems (PDSIDES)

PDSIDES is a '*knowledge-based'* computational platform that is anchored in modeling decision-related knowledge using DSP templates that are executable and reusable. Different 'knowledge-based engineering approaches' have been discussed extensively in the literature, where the focus is on the automation of the design process and not on supporting designers to make better decisions [44, 45]. The utility of the PDSIDES platform lies in its capability to provide designers with decision support during design. Through its various templates, PDSIDES facilitates the modeling of multilevel decision-making and their interactions [46] and systematic solution space visualization and exploration [36]. This is supported by predefined problem-specific information and information regarding the information and decision workflows connecting the multiple levels. The primary constructs that help realize various decisions within the PDSIDES platform are i) the Decision Support Problem (DSP) construct and ii) Ontology - the explicit formal specifications of terms used in the PDSIDES platform to formally represent the knowledge. In PDSIDES, DSPs are represented as computational decision templates called DSP templates used to model decision-making. As depicted in Figure 2, DSP templates - specifically cDSP templates, are modularized to separately capture the problem-specific declarative knowledge and the domain-independent procedural knowledge related to the procedure for solving the problem. The modules in the cDSP template, such as goals, variables, parameters, preferences, constraints, objectives, and responses, capture declarative knowledge. The analysis module captures the procedural knowledge required to execute the cDSP template. The computational environment for executing the cDSP template, DSIDES (Decision Support in the Engineering Systems) [47], is integrated into PDSIDES. The response module of the cDSP template stores the output results of the execution of the cDSP template. The use of ontologies, modularization of the DSP construct, and separation of declarative and procedural knowledge facilitate the execution and reuse of the templates in the PDSIDES platform. These templates are also editable and customizable, allowing adding additional functionalities as required. Using ontologies also helps facilitate knowledge sharing, population, and retrieval in the PDSIDES platform.

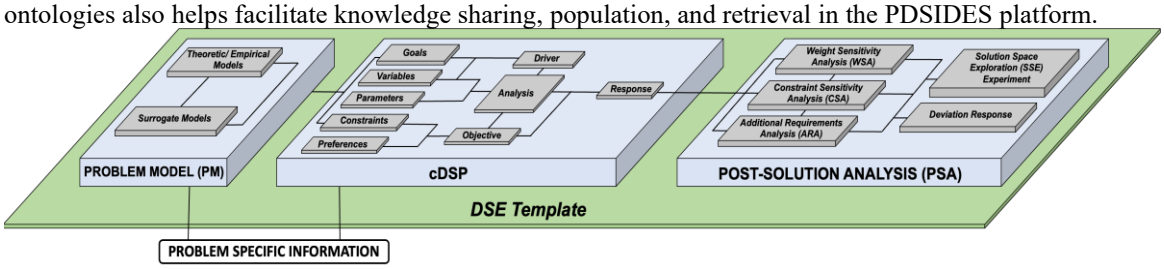

FIGURE 2: Modeling decision-making using templates, sub-templates, and modules in PDSIDES platform

In PDSIDES, the identification of satisficing solutions by solution space visualization and exploration is supported using the Design Space Exploration (DSE) template [36] depicted in Figure 2. The DSE template is composed of three separate sub-templates: i) Problem Model (PM) sub-template, ii) cDSP template, and iii) Post Solution Analysis (PSA) sub-template. Each of these sub-templates is composed of different modules that help capture declarative and procedural knowledge. The PM sub-template is composed of i) the theoretical/empirical model module that captures declarative knowledge in the form of models relating the problem-specific variables and responses and ii) the surrogate modeling module that provides designers

access to surrogate modeling tools and techniques that help develop surrogate or reduced-order models, if required. The PSA sub-template facilitates various computations, analyses, and visualization associated with the cDSP template, such as i) the creation of different design scenarios for executing the cDSP template using the Solution Space Exploration (SSE) experiment module, ii) the determination of the desired solution region using the Weight Sensitivity Analysis (WSA) module, iii) estimation of the sensitivity of cDSP responses to changes in constraint limits using Constraint Sensitivity Analysis (CSA) module, iv) other relevant post solution computations specific to the design problem, using the Additional Requirements Analysis (ARA) module, v) computation and storage of deviation of goals from their targets using the Deviation Response module, and vi) visualization and exploration of the solution space using ternary plots, by employing the ternary plot sub-module build into the PSA sub-template. The PSA sub-template produces outputs such as sensitivity values, deviation values, ternary plots, and so on that support designers in making decisions. The interactions among different decision models in PDSIDES in terms of information and decision flows can be modeled using interaction templates as presented in [46]. The PDSIDES platform also allows designers to create new templates, edit and customize existing ones, and use existing ones by modifying their parameters. For more details on PDSIDES, readers are directed to [36], [41], and [46]. The PDSIDES platform, with its various templates, sub-templates, and modules described above, is used to formulate and execute the cDSPs and explore the solution space across interacting levels in the information-decision framework presented below. The framework structure is depicted in Figure 3 and is described in Section 3.2. The use of the framework and the PDSIDES platform is discussed in Section 3.3.

3.2. Structure of the Information-Decision Framework

The framework comprises two distinct parts, as depicted in Figure 3. They are:

1) Decision models formulated for each level in a multilevel system, denoted in this paper as Levels 'n,' 'n+1', and so on, to generalize interactions between any two consecutive decision levels and
2) Interaction Space

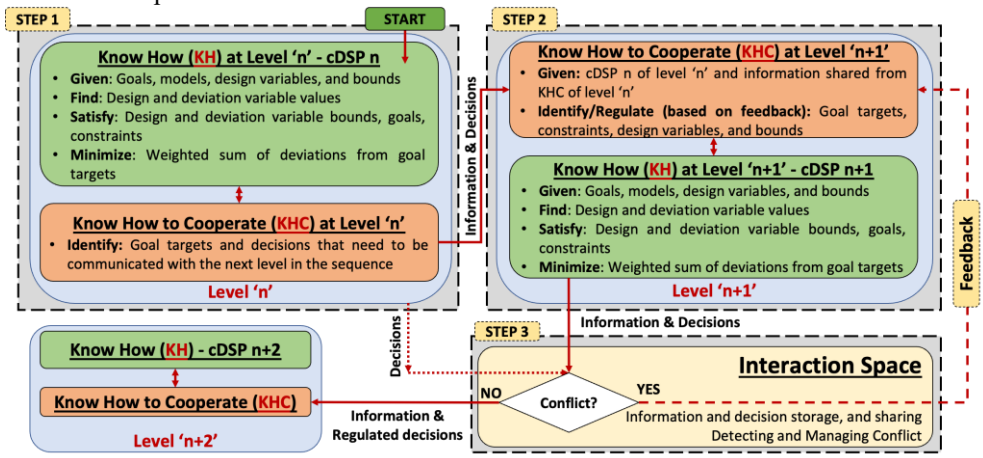

FIGURE 3: Information-Decision framework to facilitate cooperative decision-making and support multilevel, top-down co-design of product, material, and manufacturing processes

3.2.1. Decision model of interacting levels

In the framework, multilevel decision-making is represented using simulation-based decision models. The modeling of the interactions of the multilevel decision models is inspired by the human-assistance system interaction model described by Lemoine and co-authors [43]. The foundational concepts of this interaction or cooperation model are based on the Know-How (KH) and Know-How-to-Cooperate (KHC) constructs defined by Lemoine and co-authors for interacting decisional entities in a system [43].

a. KH deals with collecting level-specific information to support decision-making at a level without considering exchanges with other interacting levels.
b. KHC is concerned with understanding decision-making at interacting levels and exchanging pertinent information between the interacting levels to support cooperative decision-making.

The KH and KHC constructs are introduced by Millot and Lemoine [43] to establish generic concepts for human-machine cooperation. Since then, these constructs have been widely used in the fields of air traffic control [48], manufacturing [43, 49], and robotics [50] to facilitate human-human and human-machine cooperation. The above applications showcase the KH and KHC construct's generic nature and utility in facilitating cooperation between interacting levels through information sharing. Using these constructs, the

designer can systematically identify the information required for multilevel decision-making and the ones that need to be shared for improved cooperation between interacting levels. These characteristics make these constructs suitable to be adapted as mental models in the proposed information-decision framework to help the designers model multilevel interactions and collaboration in the decision model at each level. As depicted in Figure 3, the decision model of each level in the system is composed of the KH and KHC constructs. The KH construct allows decision-makers to model multilevel decision-making. The KHC construct enables decision-makers to identify information and decisions specific to a level or its interacting levels that can be modified, controlled, or shared to achieve improved cooperation between the interacting levels.

In this paper, KH corresponding to a level is modeled as a cDSP [40], given the possibility of each level having multiple conflicting objectives to achieve. In cDSP, both traditional mathematical programming and goal programming concepts are incorporated, enabling the exploration of satisficing design solutions for multiple conflicting goals. As depicted in Figure 4, the Given, Find, Satisfy, and Minimize keywords in the cDSP help capture information related to the problem, thus making the cDSP construct generic. The designer emphasizes achieving the goal targets defined in the cDSP as closely as possible by exploring the solution space. In the KH construct, level-specific information such as i) goals and goal targets, ii) variable bounds, and iii) constraints are used to make decisions at the respective levels. The goals are explicitly specified for the first design level. The goals are propagated inversely from higher levels in the design hierarchy for the remaining levels.

Given

- Well-established mathematical models for the problem at hand
- Goal and goal target values (G_i)
- The system parameters:

m	number of design/system variables,
j	number of system goals,
q	equality constraints,
r	inequality constraints,
$q + r$	number of system constraints,
$g_i(X_P)$	system constraint function

Find

a. System variables (X_P): Values of independent system variables, where $P = 1, 2, 3, \ldots, m$

b. Deviation variables (d_i^+, d_i^-): Values of deviation of the goal values from their target values (indicates the extent to which goals are achieved), where $i = 1, 2, 3, \ldots, j$

Satisfy

a. System Constraints (must be satisfied for solutions to be feasible and can be linear or non-linear)

$$g_i(X_P) = 0, \text{ where } i = 1, 2, 3, \ldots, q$$

$$g_i(X_P) \geq 0, \text{ where } i = q + 1, \ldots, q + r$$

b. System Goals (need to achieve a specified target value and can be linear or non-linear)

$$A_i(X_P) + d_i^- - d_i^+ = G_i, \text{ where } i = 1, 2, 3, \ldots, j$$

c. Bounds (Upper and lower limits for the system variables)

$$X_P^{min} \leq X_P \leq X_P^{max}, \text{ where } P = 1, 2, 3, \ldots, m$$

$$d_i^+, d_i^- \geq 0,\ d_i^+ * d_i^- = 0, \text{ where } i = 1, 2, 3, \ldots, j$$

Minimize

Deviation function: A function that quantifies the deviation of the system performance from that implied by the set of goals and their associated relative weights.

$$\textbf{Min } Z = \sum \boldsymbol{W_i}(\boldsymbol{d_i^+ + d_i^-})$$

where $i = 1, 2, 3, \ldots, m$, $0 \leq W_i \leq 1$, and $\sum W_i = 1$

FIGURE 4: Capturing problem-specific information using the keywords of the compromise-Decision Support Problem (cDSP) construct [40]

In PDSIDES, the decision-making Know How (KH) at a level is modeled using the PM sub-template and cDSP template. Level-specific information, including satisficing solutions identified for the specific level, is created using i) the PSA sub-template and ii) the responses stored in the response module of the cDSP template. The information generated is shared with related levels using interaction templates. The response module of the cDSP template and the PSA sub-template constitute the Know How to Cooperate (KHC) at a level in the framework.

3.2.2. Interaction Space

The interaction space is the domain that allows two major tasks to be performed using the framework. The first task is the storage and sharing of level-specific decisions and information. The second task is detecting and managing design conflicts between decisions at interacting levels. The designer uses stored information and decisions to detect and quantify design conflicts and manage these conflicts by i) identifying possible means for the interacting levels to collaborate and ii) providing corrective feedback. The procedure used to detect and quantify conflicts, identify potential corrective feedback, and its implementation in PDSIDES is discussed in the next section.

3.3. Decision support using the framework and use of the PDSIDES platform to model multilevel decision-making and their interactions, explore the solution spaces, and detect and manage conflicts

The use of the framework is explained in terms of the decisions made and the flow of information and decisions between interacting levels – Levels n, n+1, and n+2, as depicted in Figure 3. The framework involves the execution of three steps – Steps 1, 2, and 3. The decision-making in the framework takes place in Steps 1, 2, and 3. The decision workflow- the order in which decisions are made and their interconnections, is represented using the arrows connecting the steps. This represents the procedural knowledge aspect concerned with how the information is transformed and how the transformation is executed via a decision workflow. The necessary information to make decisions in Steps 1, 2, and 3 represents the problem-specific declarative knowledge concerned with what information gets transformed. The problem-specific declarative knowledge is depicted by the information and decision flows connecting the steps. Steps 1, 2, and 3 and the flow of information and decisions in the framework are described as follows.

Step 1: The KH of Level 'n' concerned with the product requirements at the top of the design hierarchy is formulated using level-specific information - declarative knowledge, such as goals ($G_{J,n}$, where 'J' - goal index and J = 1, 2,…, j), constraints (C_n), design variables ($X_{P,n}$, where P - design variable index and P = 1, 2,…, m) design variable bounds ($X_{UB,P,n}$ – upper bound and $X_{LB,P,n}$ – lower bound) and models relating the goals and design variables. At this level, goals are specified explicitly based on product performance requirements identified in terms of mechanical property goals. The product designer, the decision-maker at Level 'n,' uses this information and the cDSP construct to formulate and solve the DSP of Level 'n.' The feasible solutions that satisfy the bounds and constraints are identified by exercising the cDSP 'n' for different design scenarios, where each design scenario describes a specific combination of the designer's preference for the various goals expressed in terms of the weights assigned to the goals; see [35] for more details. From the feasible solutions, the designer identifies a collection of satisficing solutions referred to as a 'ranged set of satisficing solutions.' The ranged set of satisficing solutions identified 'satisfices' and 'suffices' the designer's requirements for the multiple goals. A ranged set of satisficing solutions for cDSP 'n' are identified through the ternary plot-based visualization of the feasible solution space and its exploration by setting acceptable thresholds for the multiple conflicting goals. The satisficing solution space identified is further explored to select a solution that fulfills the designer's preference for the goal values at Level 'n.' A more detailed discussion on visualization and exploration of the feasible solution space using ternary plots to identify a satisficing solution is provided in Section 4. The above decision – the satisficing solution identified, along with the information regarding the KH of Level 'n,' is passed to the KHC of Level 'n,' from where they are then propagated to the KHC of Level 'n+1' that corresponds to the next level in the inverse design sequence. Therefore, there exists propagation of goals between interacting levels in an inverse manner. To summarize, in Step 1, the product designer formulates and solves the cDSP at Level 'n' and explores the feasible solution space to identify a satisficing solution that is propagated as the goal target for the next design level in the inverse sequence, Level 'n+1.'

Step 2: The materials designer, the decision-maker at Level 'n+1,' uses the decision propagated to its KHC from Level 'n' to identify goals and goal targets to work towards. The KH of Level 'n+1' concerned with meeting the materials requirements identified and propagated from Level 'n' is provided with level-specific information - declarative knowledge, such as goals ($G_{J,n+1}$), constraints (C_{n+1}), design variable ($X_{P,n+1}$), design variable bounds ($X_{UB,P,n+1}$ – upper bound and $X_{LB,P,n+1}$ – lower bound) and models relating the goals and design variables, as in Step 1. The final processing in the manufacturing process chain influences the goals at Level 'n+1.' Similar to Step 1, the materials designer uses level-specific information to formulate and solve cDSP 'n+1' and identify feasible solutions. The ranged set of satisficing solutions for Level 'n+1' are identified using a ternary plot-based feasible solution space visualization. Acceptable thresholds for the multiple conflicting goals are identified, and the solution space within the ternary space is explored. The materials designer identifies a satisficing solution from the ranged set that fulfills their preference for the goal values of Level 'n,' achieved by mapping the goal values at Level 'n+1' as design variable values for Level 'n.' The above decision – the chosen satisficing solution and corresponding goal values of Level 'n' are then propagated to the interaction space, where decisions at the interacting levels are compared to detect conflicts. In Step 2, the materials designer, using the information propagated down from Level 'n' and level-specific information, formulates and solves the cDSP at Level 'n+1' to identify satisficing solutions. The materials designer further explores the satisficing solution space to identify satisficing solutions at Level 'n+1.' The corresponding Level 'n' goal values are subsequently propagated to the interaction space to detect conflicts.

In PDSIDES, Steps 1 and 2 are modeled using separate instances of the DSE template. In the DSE template instances, the declarative knowledge in Steps 1 and 2 is captured using the goals, variables,

constraints, parameters, preferences, and objectives modules of the cDSP template. Additional declarative knowledge in the form of models relating the variables and goals for both steps is captured in the PM sub-templates theoretical/empirical model module. If no models are available, surrogate models are developed using the surrogate modeling module of the PM sub-template. Using the procedural knowledge in the analysis module of the cDSP template, the cDSPs in Steps 1 and 2 are executed to generate feasible solutions. The visualization and exploration of the solution space at both levels are supported using i) the SSE experiment and WSA modules of the PSA sub-template and ii) the ternary plot sub-module built into the PSA sub-template. The information and decision flow between the separate instances of the DSE templates for Steps 1 and 2 are established using the interaction templates in PDSIDES.

Step 3: The decisions made at Levels 'n' and 'n+1' in Steps 1 and 2 are shared with the interaction space as depicted by the dotted red line from Level 'n' and the solid red line from Level 'n+1' to interaction space. The decisions are jointly analyzed in the interaction space to detect and manage design conflicts. A flowchart representing the sequence of computations performed as part of Step 3 is shown in Figure 5.

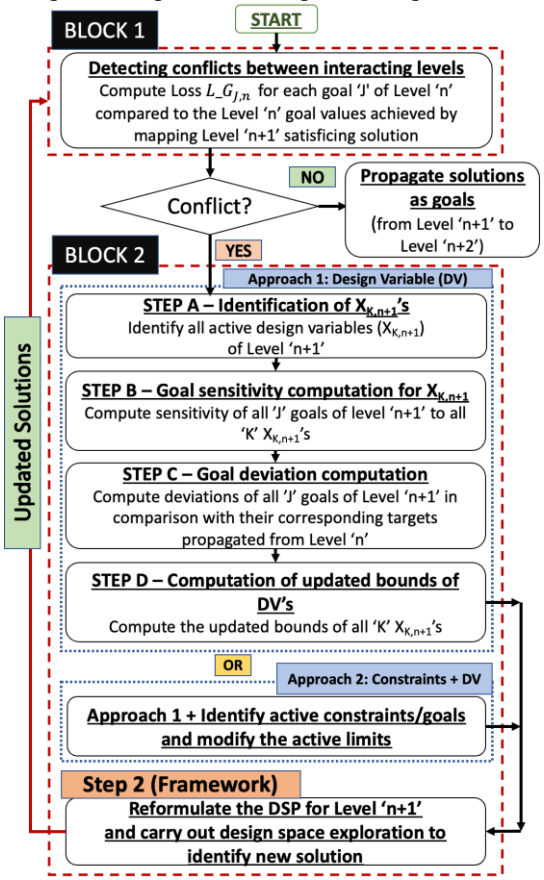

FIGURE 5: Steps involved in detecting and managing design conflicts between decisions at interacting levels

Step 3 comprises two blocks, as described below.

Block 1 - Detecting design conflicts between decisions at interacting levels

In this block, the loss in each goal 'J' of Level 'n' ($L\_G_{J,n}$) is computed as per Equation 1. The loss metric is quantified by comparing values achieved for each goal 'J' of Level 'n' ($G_{J,n}$) identified in Step 1 to the goal values that are achieved by mapping Level 'n+1' goal values from Step 2 as design variable values for Level 'n.' The goal values achieved at Level 'n+1' are depicted as $G_{1,n+1}$, $G_{2,n+1}$ and $G_{3,n+1}$ in Figure 6. The loss metric is used to detect and quantify the extent of the conflict between interacting levels.

$$L\_G_{J,n} = \frac{G_{J,n\ satisficing} - G_{J,n\ achieved}}{G_{J,n\ satisficing}} \quad (1)$$

where $G_{J,n_{satisficing}}$ is the satisficing value of $G_{J,n}$; $G_{J,n\ achieved}$ is the value achieved for $G_{J,n}$ corresponding to the satisficing solution picked at Level 'n+1' in Step 2.

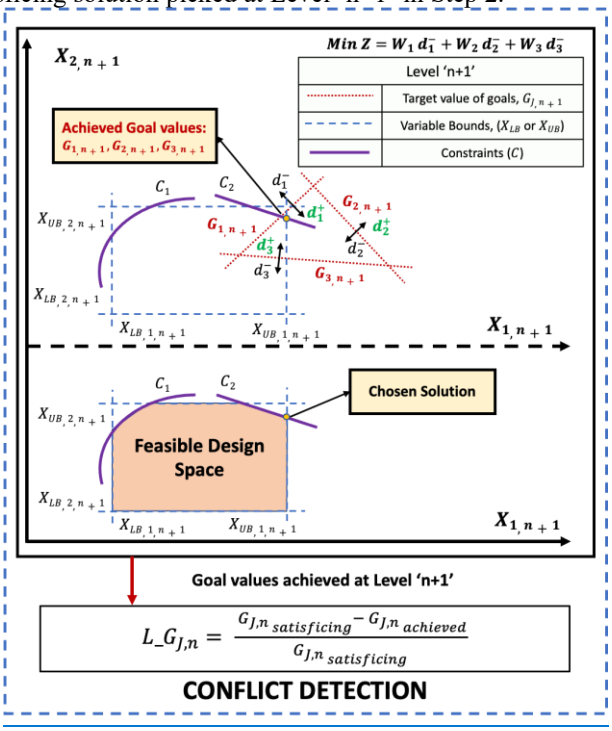

FIGURE 6: Detecting conflicts between interacting Levels 'n' and 'n+1'

Calculating the loss requires the use of the KHC of Level 'n+1', where the goal values of Level 'n+1' are mapped to the empirical models of Level 'n' goals – KHC of Level 'n+1,' to find corresponding goal values for Level 'n.' In Figure 6, given the constraints and variable bounds at Level 'n,' the achieved goal value for the maximization goal - $G_{2,n+1}$, is below its target value, indicating an underachievement as indicated by d_2^-. Hence, the best solution for Level 'n+1' does not meet all the goal targets propagated from Level 'n, resulting in a loss at Level 'n.'

In cases where the designer aims to maximize a goal, conflict occurs when the best value achieved for the goal is less than the satisficing value chosen. In such a case, the numerator of Equation 1 will be positive, resulting in a positive value for the loss metric. When minimizing a goal value is the designer's focus, conflict occurs when the best value achieved for the goal is greater than the satisficing value chosen for the goal. Consequently, the numerator of Equation 1 will be negative, resulting in a negative value for the loss metric. Hence, positive values of loss ($L\_G_{J,n}$) indicate conflict when the designer aims at maximizing the goal values. In cases where the designer seeks to minimize the goal values, negative loss values indicate conflict. The loss values are normalized, and the larger the magnitude of loss computed for any of the 'J' goals of Level 'n,' the more significant the conflict between interacting multilevel decisions. In a case where multiple conflicts are identified, the one with the largest magnitude of loss value takes priority.

Hence, in Block 1 of Step 3, the designer seeks to detect conflicts between the decisions at Levels 'n' and 'n+1' by identifying the lack of achievement of satisficing goal targets at Level 'n' due to decisions made at Level 'n+1'. If no conflicts are detected in any goals, the satisficing solution at Level 'n+1' is propagated to the next level in the inverse design sequence - Level 'n+2.' Level 'n+2' is concerned with meeting the materials requirements influenced by the second to last manufacturing process in the material processing sequence. Subsequently, Levels 'n+1' and 'n+2' in the framework become the new Level 'n and 'n+1', respectively, and Steps 2 and 3 are then re-executed. If any conflicts are detected, they are managed using Approach 1 or 2 in Block 2, as discussed below. This is continued till all the processing operations in the manufacturing sequence are accounted for. In PDSIDES, the conflict detection by computation of loss values is added as additional functionality to the ARA module of the PSA sub-template by leveraging the capability of the templates to be edited or customized.

Block 2 - Managing conflicts

Conflicts identified in Block 1 between decisions at interacting levels must be managed to achieve the required multilevel and system performance. Two approaches – Approach 1 and 2, depicted in Block 2 of Figure 5, are proposed for managing conflicts in the framework. These approaches are detailed below.

Approach 1

Step A: Block 2 starts with the identification of all active design variables at Level 'n+1' ($X_{K,n+1}$, where 'K' - index of active design variables, K= 1, 2, …, k and k<m - number of design variables as depicted in Figure 4) and active constraints (C_{n+1}). Active design variables are those with values at the upper or lower bounds.

Step B: The sensitivity of goal 'J' of level 'n+1' ($G_{J,n+1}$) to the $X_{K,n+1}$'s - $S_{J,X_{K,n+1}}$ is calculated as per Equation 2. The sensitivity computation is based on the Nominal Range Sensitivity metric, S [51, 52], depicted in Figure 7. To use Equation 2, it is assumed that the goals are monotonic and that design variables are independent.

$$S_{J,X_{K,n+1}} = \frac{G_{J,X_{UB,K,n+1}} - G_{J,X_{LB,K,n+1}}}{X_{UB,K,n+1} - X_{LB,K,n+1}} = \frac{dG_{J,X_{K,n+1}}}{dX_{K,n+1}} \quad (2)$$

where, $G_{J,X_{UB,K,n+1}}$ and $G_{J,X_{LB,K,n+1}}$ are the values of $G_{J,n+1}$ at the upper and lower bounds of $X_{K,n+1}$, respectively, for a specific combination of the remaining X_{n+1} values; and $X_{UB,K,n+1}$ and $X_{LB,K,n+1}$ are the upper bound and lower bound of $X_{K,n+1}$, respectively.

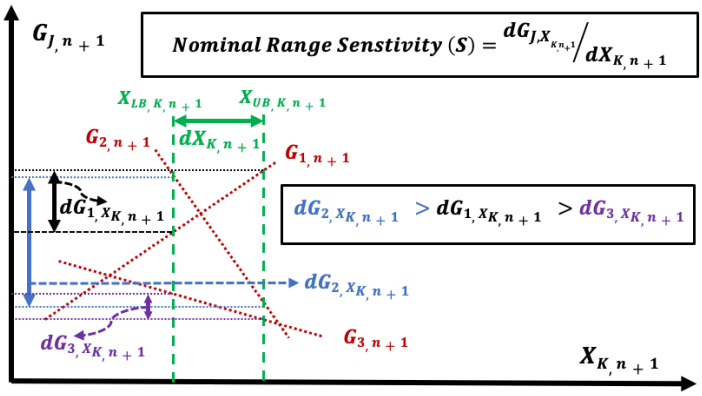

FIGURE 7: Sensitivity of goals of Level 'n+1' to active design variable $X_{K,n+1}$

The sensitivity computation is performed for various combinations of all the remaining X_{n+1} values at their upper, lower, or nominal (average value of the variable bounds) values. The largest of the sensitivity values computed for a goal 'J' in magnitude is considered its sensitivity to the specific $X_{K,n+1}$. Higher sensitivity values indicate that a slight change in $X_{K,n+1}$ value can significantly change the goal value, enabling the designer to achieve improved performance by modifying $X_{K,n+1}$ by a small amount. The above scenario is illustrated in Figure 7, where the nominal range sensitivity is the highest for Goal 2 ($G_{2,n+1}$) amongst all three goals of Level 'n+1', since for a given change in $X_{K,n+1}$ values - dX_{K,n_1}, Goal 2 has the most significant change in its value.

This corresponds to a situation in the physical system where a slight increase in resource utilization will help the designer realize more significant performance improvements. The sensitivity computation is repeated for all the remaining $G_{J,n+1}$'s to estimate the sensitivity of all 'J' goals of Level 'n+1' to a particular $X_{K,n+1}$. As discussed above, Step B is repeated for all $X_{K,n+1}$'s identified in Step A.

Step C: Next, the deviations of the achieved values of all 'J' goals at Level 'n+1' compared to their targets from Level 'n' are computed using Equation 3.

$$D_{G_{J,n+1}} = G_{J,n+1\,target} - G_{J,n+1_{achieved}} \quad (3)$$

where, $D_{G_{J,n+1}}$ is the deviation of $G_{J,n+1}$; $G_{J,n+1\,target}$ is the propagated target values of $G_{J,n+1}$; and $G_{J,n+1_{achieved}}$ is the value of $G_{J,n+1}$ achieved from the satisficing solution chosen in Step 2.

The $D_{G_{1,n+1}}$, $D_{G_{2,n+1}}$ and $D_{G_{3,n+1}}$ values at Level 'n+1' that are computed as per Equation 3 are equivalent to the d_1^+, d_2^-, and d_3^+ values in Figure 6. It is observed that d_1^+ and d_3^+ are over achievements that positively

influence the maximization of goals $G_{1,n+1}$ and $G_{3,n+1}$ with goal values greater than their targets. However, d_2^- represents an under-achievement that is deleterious for the maximization goal $G_{2,n+1}$ with the goal value lower than the target. The deviation function of the cDSP for Level 'n+1' looks at minimizing the weighted sum of under-achievements of the maximization goals - d_1^-, d_2^-, and d_3^- from the target values as depicted by function Z in Figure 6. Hence, any change that can help achieve a solution that reduces the under-achievement of goals is beneficial for the scenario represented in Figure 6.

Step D: The updated bound of $X_{K,n+1}$, identified in Step A, is computed in this step. First, the update required in $X_{K,n+1}$ value to achieve the target value of goal 'J' of Level 'n+1' - $U_{J,X_{K,n+1}}$ is calculated using Equation 4.

$$U_{J,X_{K,n+1}} = \frac{D_{G_{J,n+1}}}{S_{J,X_{K,n+1}}} \tag{4}$$

The above computation is also carried out for the remaining 'J-1' goals of Level 'n+1'. The rules for choosing a final update value for $X_{K,n+1}$ - $U_{X_{K,n+1}}$, from the values computed using Equation 4 for different goals are given below.

a. If $X_{K,n+1}$ is at its lower bound, the largest negative value in magnitude, if any, is chosen as the update required for $X_{K,n+1}$. Otherwise, the updated value is set to zero. A negative value is selected to reduce the active lower bound and thereby relax $X_{K,n+1}$. The largest value in magnitude is selected as it would help meet the largest goal deviations identified in Step D.
b. If $X_{K,n+1}$ is at the upper bound, the largest positive value in magnitude, if any, is chosen as the change required for that $X_{K,n+1}$. Otherwise, the updated value is set to zero. A positive value is selected as it will increase the active upper bound and thereby relax $X_{K,n+1}$. The largest value in magnitude is chosen as it would help meet the largest goal deviations identified in Step D.

Using the $U_{X_{K,n+1}}$ value, the updated bound of the $X_{K,n+1}$ ($X_{K,n+1\ Updated\ bound}$) is computed as per Equation 5.

$$X_{K,n+1\ Updated\ bound} = X_{K,n+1\ Original\ bound} + U_{X_{K,n+1}} \tag{5}$$

The updated active design variable bounds will help designers improve the solution by bringing the updated under-achievement deviation term ($d_{2,up}^-$) to zero, as depicted in Figure 8. Hence, all the goal values are either at their target values or greater. This improved solution at Level 'n+1'can potentially help mitigate or manage (reduce) conflicts computed in Block 1.

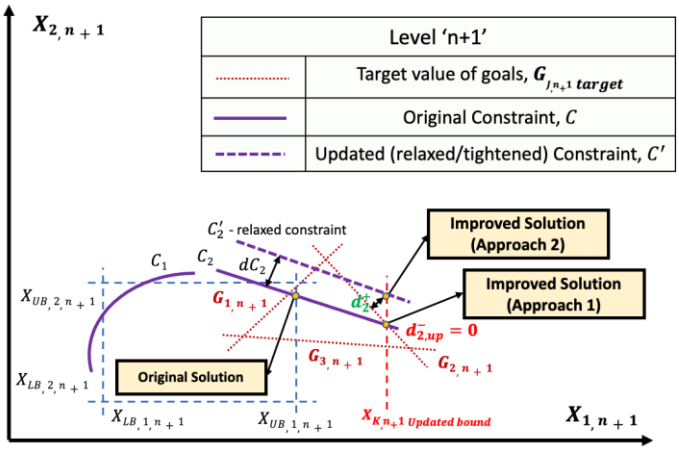

FIGURE 8: Updating active design variable bounds and constraints to achieve improved solutions corresponding to Level 'n+1'

In Approach 1, the designer seeks to manage conflicts and help achieve improved satisficing solutions closer to the goal targets by identifying active design variables and relaxing their bounds within acceptable limits. The extent of relaxation of the active variable bounds is computed by considering i) the sensitivity of the goals with respect to the active design variables and ii) the degree of underachievement of goals. The updated active design variable bounds are determined based on the extent of relaxation computed above and the designer's domain knowledge.

Approach 2

Approach 2 is used when there are both active constraints and active design variables ($X_{K,n+1}$). Here, $X_{K,n+1}$ bounds are modified as in Approach 1, and the active constraint limits are also relaxed within feasible limits based on the designer's domain knowledge. The benefit of relaxation of the limits of the active constraints along with the updating of active variable bounds can be explained using Figure 8, where the active constraint C_2 is relaxed by an amount dC_2. The above relaxation and the updated bound for the active design variable, helps achieve an improved solution at Level 'n+1'. The improved solution results in the deviation of Goal 2 - $d_{2,up}^-$ being replaced by the over achievement term d_2^+. Hence, the relaxation of the limits of the active constraints along with the modification of active variable bounds helps achieve an improved solution at Level 'n+1' that results in goal values greater than targets. This improved solution potentially aids in managing conflict computed in Block 1. Therefore, in Approach 2, the designer seeks to manage conflicts and help achieve improved satisficing solutions closer to the goal targets by modifying active design variable bounds and relaxing the active constraint limits based on the designer's domain knowledge. Changing the limits of active constraints that are not purely bound-based requires designers to perform constraint function evaluations and assess the impact on the decision support problem. Systematic approaches for constraint function evaluation are beyond the scope of the current paper and are not discussed. In this paper, we rely on the designer's domain knowledge to modify the active constraint limits.

The updated bound values of $X_{K,n+1,}$ along with the relaxed, active constraint limits, if any, are provided as corrective feedback to the KHC of Level 'n+1' to help MDC and FG. Using the information from the updated KHC, Step 2 is repeated, where the materials designer formulates an updated cDSP for Level 'n+1', followed by solution space exploration to arrive at a new solution or decision. The new solution is then propagated to the interaction space, and Block 1 of Step 3 is repeated to detect conflicts. If no conflicts are detected, the updated solution or decision – the regulated decision at Level 'n+1' is propagated as goals for Level 'n+2'. If conflicts are detected, Block 2 of Step 3 is executed to exploit further opportunities to modify active variables and constraints. If there are no possibilities of such a modification, the product designer at Level 'n' will need to reformulate the product design cDSP with new goals that are achievable and consistent with the requirements at Level 'n+1'. The entire process is repeated at all other levels with specific material requirements that correspond to the different processing operations in the sequence.

In the PDSIDES platform, conflict management, which involves i) identification of active design variables and constraints, ii) computation of sensitivity of goals to design variables, and iii) computation of updated active variable bounds and constraint limits, are functionalities that are added to the ARA module of the PSA sub-template by leveraging the capability of the templates to be edited or customized. The CSA module within the PSA sub-module can support designers in estimating the updated limits of active constraints, which is not used in this work. The updated active design variable bounds and active constraint limits are provided as new values to the constraint and variable modules of the cDSP template using the interactions template.

4. DEMONSTRATION USING HOT ROD ROLLING (HRR) TEST PROBLEM

The HRR problem is used to showcase the efficacy of the proposed framework for co-designing the hot rolled rod product, steel material, and rolling and cooling manufacturing processes. The material considered is C-Mn steels to realize round steel rods that are to be used as gear blanks to produce gears. The problem is based on the industry-inspired HRR problem presented by Nellippallil and co-authors [35]. The empirical models used for the HRR problem are provided in Tables A1 and A2 of Appendix A.

HRR of steel is a complex manufacturing process used to produce hot-rolled steel rods. It comprises a series of manufacturing processes executed sequentially, starting with reheating the input primary steel obtained from the casting unit in the form of slabs or blooms, referred to here as the 'reheating process.' This is followed by plastic deformation of the material by passing the material through several rollers in rolling mills, referred to here as the 'rolling process.' Further, cooling of the rolled product is carried out in a run-out table, referred to here as the 'cooling process.' The above thermo-mechanical processing causes microstructural evolution and macrostructural changes in the steel material, resulting in hot-rolled steel rods with specific microstructural characteristics and corresponding mechanical properties [35], as depicted in Figure 9.

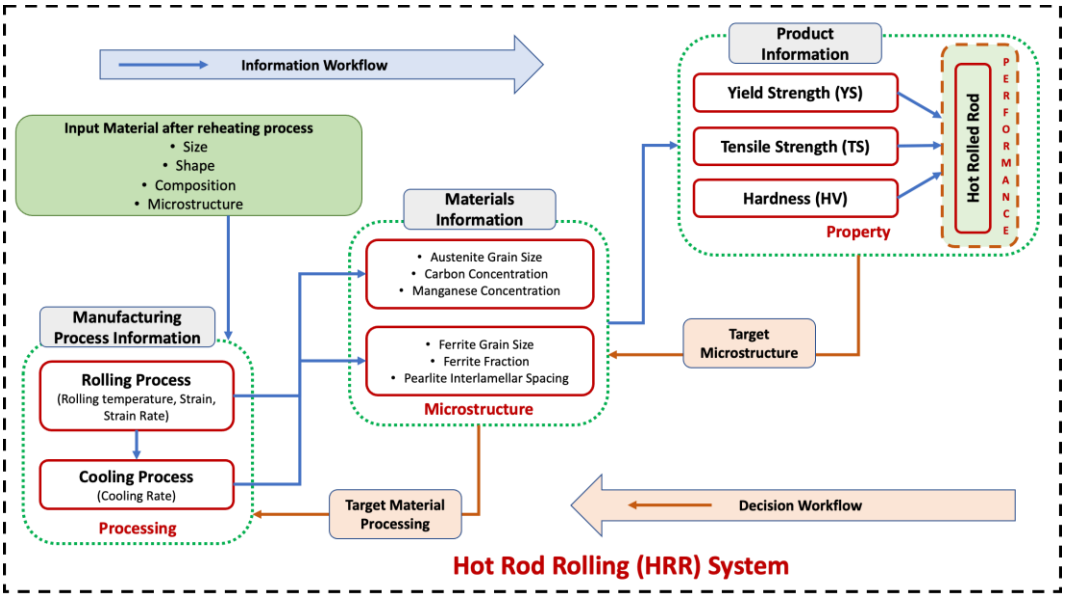

FIGURE 9: Information and decision flow across the HRR system that involves product, materials, and manufacturing processes.

The performance requirements of the hot-rolled steel rods are identified in terms of the target mechanical properties values of the gears to be produced using the rods. Realizing hot rolled rods with targeted mechanical properties requires a collective consideration of the material microstructure and composition and its processing. In showcasing the framework's utility, we consider the rolling and cooling manufacturing processes, the resulting microstructure of the steel material, and the resultant steel rod products. In Figure 9, we depict decision workflows across three levels of decision-making: i) Level 1 - considering the information and decision flows between product and materials: where decisions are made with regard to the material microstructure at the end of the cooling process, in order to meet the mechanical property/performance requirements of the product, ii) Level 2 - considering the information and decision flows between materials and manufacturing process: where decisions are made regarding materials processing during the cooling process and material microstructural characteristics at the start of the cooling process to meet the microstructural requirements at the end of the cooling process (identified at Level 1), and iii) Level 3 considering the information and decision flows between materials and manufacturing process: where decisions are made regarding the materials processing during the rolling process to meet the microstructural requirements at the start of the cooling process (identified at Level 2). The decision-making at these levels is represented using simulation-based decision models using cDSP's. Through the multilevel decisions, we achieve the co-design of the hot rolled rod product, steel material, and hot rolling and cooling manufacturing processes.

Decision-making at the different levels in HRR systems is in itself a challenging task. This involves choosing the appropriate combination of design variables values, given several conflicting goals or objectives that must be achieved while satisfying several constraints and bounds. With the decision-making in the HRR system taking place sequentially, the output of one level - a result of the decisions made at the level, acts as the input for the next level. Hence, decisions are interconnected based on the forward sequential information flow from one level to the next. In Figure 9, we depict this information flow between decisions across the different levels in the HRR system. The forward information flow starts with the rolling process, receiving input data about the characteristics of the steel in terms of shape, size, composition, and microstructure after the reheating process. Decisions are made regarding the rolling process variable values using these inputs and other rolling-specific data. These decisions include identifying the values for rolling temperature, strain, strain rate, and so on that determine the intermediate product's resultant microstructure, shape, and size. The microstructure information is subsequently propagated as input to the cooling process. The decisions made during the cooling process determine the final material microstructural characteristics, such as steel phase fractions and grain size, which determine the mechanical properties of the hot-rolled rod product and its performance.

In this paper, to showcase the proposed framework's efficacy, we only consider the potential design conflicts arising from the interactions between the decisions made at Levels 1 and 2. At Level 1, three

important mechanical properties, Yield Strength (YS), Tensile strength (TS), and Hardness (HV) of the hot-rolled rod, are considered, as they are intended to be used subsequently as gear blanks to produce gears. Using the GoID approach, the inverse decision workflow begins with the decisions at Level 1 that are directed toward achieving maximum YS, TS, and HV values. The target values for these goals are specified based on the mechanical property requirements of the gear. The decisions at Level 1 regarding the microstructure characteristics of the hot rod rolled rod, defined by ferrite grain size, ferrite fraction, and pearlite interlamellar spacing, are propagated to Level 2 as its targets. Hence, at Level 1, the product-material interactions are considered.The decisions at Level 2 are directed toward identifying the right combination of design variable values for austenite grain size after the rolling process and cooling rate during the cooling process that will help realize the target microstructures. Hence, at Level 2, the materials-manufacturing process interactions are considered. By considering Levels 1 and 2, we are able to showcase the co-design of the products, materials, and manufacturing processes. The set targets at Level 2 may not be realized during exploration due to the constraints under which the Level 2 decisions are made. A satisficing solution is identified after exploring the generated solution space. If the solutions identified at Level 2 differ from those already identified at Level 1, design conflicts between decisions made at Levels 1 and 2 arise. The above conflict between the decision made at Levels 1 and 2 and the use of the framework to manage this conflict is demonstrated below. We start by identifying the Levels 'n' and 'n+1', discussed in Section 3.2. In the problem defined, Level 'n' refers to Level 1, and Level 'n+1' refers to Level 2.

Step 1: The formulation of cDSP for Level 1 is carried out by the product designer using microstructure and mechanical property relations - empirical models, design variables ($X_{P,Level\ 1}$), bounds ($X_{UB,P,Level\ 1}$ – upper bound and $X_{LB,P,Level\ 1}$– lower bound), constraints ($C_{Level\ 1}$), and mechanical property goals ($G_{J,Level\ 1}$) of the hot rolled rod. This is the KH of Level 1, passed to its KHC, summarized in Table 2. The KHC of Level 1 is further propagated to the KHC of Level 2, outlined in Table 3. In the PDSIDES platform, the microstructure-mechanical property relations are stored in the PM sub-template, and the Level l design variables, bounds, constraints, and goals are captured using the corresponding modules in the cDSP template. Here, Level 1 goals are set to maximize the YS, TS, and HV values as close to the target values of 330 MPa, 750 MPa, and 170, respectively. The cDSP formulation for Level 1 is given in Table A3 of Appendix A.

A set of design solutions that meet the conflicting design goals at Level 1 is identified by executing the above cDSP formulation for 25 different design scenarios, named A to Y. The set of solutions corresponding to the 25 design scenarios defines the solution space at Level l. The scenarios are defined by the weights assigned for the deviations of goals from the target values in the deviation function. The weights corresponding to each design scenario are identified by uniformly sampling the design space and based on the designer's judgment to effectively capture the HRR problem's solution space. The deviation function formulated captures the designer's preference while solving the particular cDSP. For example, a weight of 1 to the first goal and zero to the others indicates that the designer's preference using the deviation function formulated is to achieve goal 1 to the target as closely as possible. These scenarios and appropriate satisficing solution space for the goals at Level 1 are visualized and identified using ternary plots. The search for a satisficing solution space for the goals begins by specifying acceptable threshold values for each goal. YS is the mechanical property of focus in this paper. Therefore, the satisficing solution space is defined by the thresholds: YS ≥ 290 MPa, TS ≥ 500 MPa, and HV ≥ 130. These acceptable threshold values are marked on the ternary plots of the individual goals to identify satisficing solution space for each goal; see Figures 10a, 10b, and 10c. The ternary plots indicating the satisficing solution space for the goals at Level 1 are superimposed to identify the common satisficing solution region and the corresponding common design scenarios at Level 1, see Figure 10d. The ternary plots for YS, TS, and HV goals, along with the superposed plot for Level 1, are shown in Figures 10a, 10b, 10c, and 10d, respectively. The solution space in the direction of the arrows, starting from the yellow dashed line in Figure 10a, indicates the satisficing solution space for YS. The entire solution space for TS and HV is satisficing, as indicated by the arrows in Figures 10b and 10c. The highlighted region in Figure 10d depicts the satisficing solution space for Level 1.

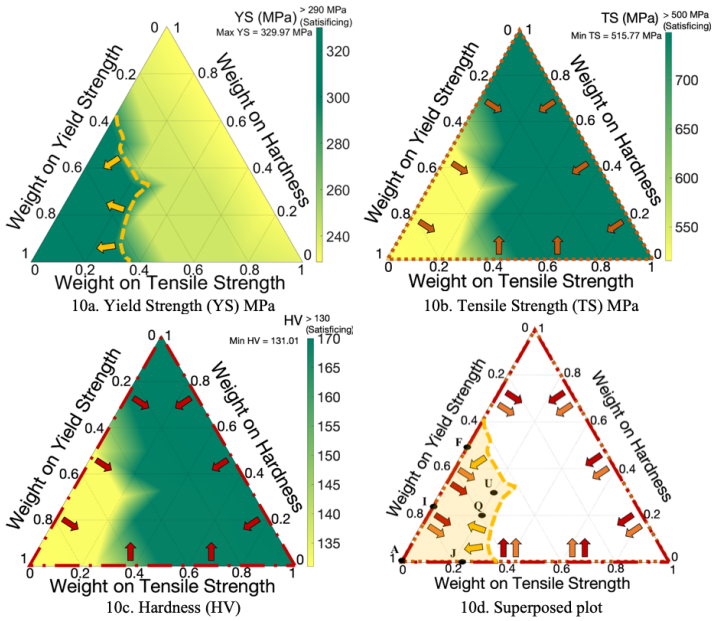

FIGURE 10: Ternary plots for 10a. YS, 10b. TS, 10c. HV, and 10d. Superposed plot for Level 1

Level 1 goal values at different design scenario points within this satisficing solution space - scenarios A, F, I, J, Q, and U listed in Table 1 are evaluated in accordance with the designer's preference. The designer's preference is to select a solution that results in goal values near the target values for all the goals. Based on the preference, the designer picks the satisficing solution corresponding to design scenario U as there is no clear preference among these five alternatives. This choice results in the following goal values: YS = 329.96 MPa, TS = 520.79 MPa, and HV = 131.84. The design variables values corresponding to the above decision (X_f = 0.883, d_α = 8 μm, S_0 = 0.15 μm, Si = 0.3%, N = 0.009%, and Mn = 1.5 %) are passed to the KHC of Level 1 summarized in Table 2, which will, in turn, be propagated to the KHC of Level 2 summarized in Table 3. At Level 2, the materials designer uses the X_f, d_α, and S_0 values from its KHC as goal targets, thereby promoting cooperation with Level 1.

TABLE 1: Level 1 solutions

Design Scenario	Weight on Goals (W_J)			Goals ($G_{J,n}$)			Design Variables (X_n)		
	W_1	W_2	W_3	$G_{1,1}$ YS(MPa)	$G_{2,1}$ TS(MPa)	$G_{3,1}$ HV	X_f	d_α (μm)	S_0 (μm)
A	1	0	0	329.97	515.77	131.01	0.900	8.00	0.15
F	0.5	0	0.5	329.96	520.79	131.84	0.883	8.00	0.15
I	0.75	0	0.25	329.96	520.79	131.84	0.883	8.00	0.15
J	0.75	0.25	0	329.96	520.79	131.84	0.883	8.00	0.15
Q	0.6	0.2	0.2	329.96	520.79	131.84	0.883	8.00	0.15
U	0.5	0.2	0.3	329.96	520.79	131.84	0.883	8.00	0.15

TABLE 2: Information contained in the KHC of Level 1

Sl. No.	Information
a.	Level 1 design variable values (corresponding to the satisficing solution picked) that need to be propagated to Level 2 as its goal targets: X_f = 0.883, d_α = 8.000 μm, S_0 = 0.150 μm, Si = 0.300 %, N = 0.009 % and Mn = 1.500 %.
b.	Microstructure-mechanical property models from cDSP of Level 1.

TABLE 3: Information contained in the 'initial KHC' of Level 2

Sl. No.	Information
a.	Goal target values propagated from Level 1: X_f = 0.883, d_α = 8.000 μm, S_0 = 0.150 μm.
b.	Microstructure-mechanical property models from cDSP of Level 1.

Step 2: The cDSP for Level 2 is formulated by the materials designer using information regarding models relating to processing and microstructure; design variables ($X_{P,Level\ 2}$), and their bounds ($X_{UB,P,Level\ 2}$ – upper bound and $X_{LB,P,Level\ 2}$ – lower bound); constraints ($C_{Level\ 2}$), and goals ($G_{J,Level\ 2}$). The initial cDSP formulation for Level 2 and the empirical models used in this formulation are provided in Tables A3 and A2, respectively, of Appendix A. In the PDSIDES platform, the processing-microstructure relations are stored in the PM sub-template. Level 2 design variables, bounds, constraints, and goals are captured using the corresponding modules in the cDSP template. The goals for this level are set to maximize X_f and minimize d_α and S_0 values. This choice is based on a comparison of the target values from the KHC of Level 2 - design variable values corresponding to the design scenario U chosen in Step 1 and design variable bounds from the KH of the same level, as specified by the variable bound values in the cDSP formulation for Level 2 in Table A3 of Appendix A.

In a manner similar to *Step 1*, a set of satisficing design variable values that meet the conflicting goals is identified by executing Level 2 cDSP formulation for the 25 different design scenarios, named A to Y. The appropriate satisficing solution space for Level 2 is visualized using ternary plots. The satisficing solution space is defined by $d_\alpha \leq 25.1\mu m$, $S_0 \leq 0.155\mu m$, and $X_f \geq 0.7$. The ternary plots for d_α, S_0, and X_f are shown in Figures 11a, 11b, and 11c, respectively, and Figure 11d shows the superposed plot for Level 2 corresponding to the initial solutions.

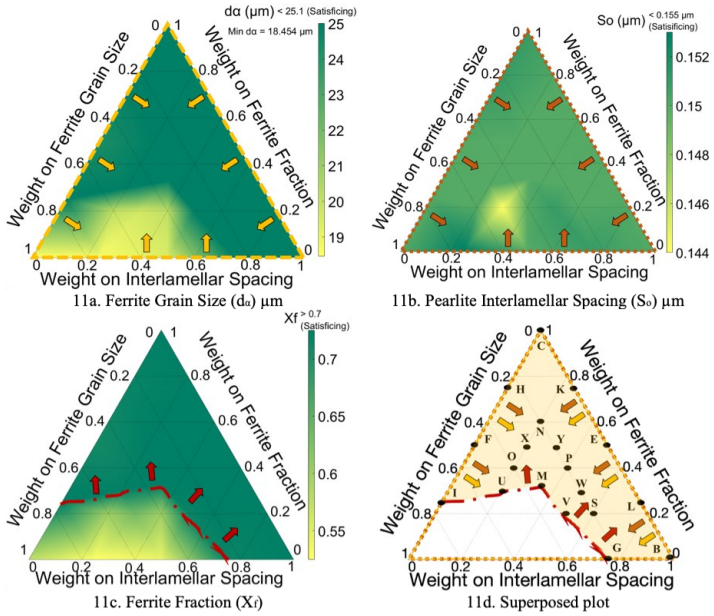

FIGURE 11: Ternary plots for goals dα (11a), S_0 (11b), X_f (11c), and the superposed plot (11d) for Level 2 corresponding to the initial Level 2 solutions

The yellow dashed line in Figures 11a and 11d, the orange dotted lines in Figures 11b and 11d, and the red chain line in Figures 11c and 11d represent the satisficing boundaries of d_α, S_0, and X_f, respectively. The arrows indicate their feasible directions. The overall satisficing solution space corresponding to the initial Level 2 solution is highlighted in Figure 11d. The goal values corresponding to different design scenarios that fall in the satisficing space are listed in Table 4. The microstructure goal values achieved are mapped to the microstructure-mechanical property relations of Level 1 from KHC of Level 2, to compute the corresponding Level 1 goal values. For example, for design scenario Y in Table 4, the goal values $d_\alpha = 25.01$ μm, $S_0 = 0.15$ μm, and $X_f = 0.72$ of Level 2, when mapped to the empirical relations between mechanical properties and microstructure at Level 1, will result in YS = 279.81 MPa, TS = 502.45 MPa and HV = 139.57. This is repeated for all design scenarios listed in Table 4. The designer's preference is to pick a design scenario in Table 4 that yields the value closest to the satisficing targets of the goal of primary importance (YS) picked in *Step 1* while still meeting the remaining two goals (TS and HV). A solution is selected using the computed values of the Level 1 goals that correspond with the Level 2 goal values and after considering the designer's preference. The solution corresponding to design scenario Y is chosen as the Level 2 solution. The above solution and corresponding computed goal values in Level 1 are propagated to the interactions space to compare and detect conflicts in the next step.

TABLE 4: Initial Level 2 solutions

Design Scenario	Weight on Goals (W_J)			Goals ($G_{J,n+1}$)			Design Variables (X_{n+1})			
	W_1	W_2	W_3	$G_{1,2}$ d_α (μm)	$G_{2,2}$ S_0 (μm)	$G_{3,2}$ X_f	C (%)	Mn (%)	d_γ (μm)	CR (°C/s)
B	0	1	0	25.01	0.15	0.72	0.18	1.46	30.01	0.27
C	0	0	1	25.01	0.15	0.72	0.18	1.45	30.01	0.27
E	0	0.5	0.5	25.01	0.15	0.72	0.18	1.46	30.01	0.27
F	0.5	0	0.5	24.31	0.15	0.71	0.19	1.50	30.00	0.26
G	0.25	0.75	0	25.01	0.15	0.72	0.19	1.50	30.01	0.24
H	0.25	0	0.75	25.01	0.15	0.72	0.19	1.50	30.01	0.24
I	0.75	0	0.25	25.01	0.15	0.72	0.18	1.46	30.01	0.27
K	0	0.25	0.75	25.01	0.15	0.72	0.18	1.46	30.01	0.27
L	0	0.75	0.25	25.01	0.15	0.72	0.18	1.46	30.01	0.27
M	0.33	0.34	0.33	25.01	0.15	0.72	0.18	1.46	30.01	0.27
N	0.2	0.2	0.6	25.01	0.15	0.72	0.18	1.46	30.01	0.27
O	0.4	0.2	0.4	25.00	0.15	0.72	0.18	1.50	30.00	0.24
P	0.2	0.4	0.4	25.01	0.15	0.72	0.18	1.46	30.01	0.27
S	0.2	0.6	0.2	25.01	0.15	0.72	0.18	1.46	30.01	0.27
U	0.5	0.2	0.3	25.00	0.15	0.72	0.18	1.50	30.00	0.24
V	0.3	0.5	0.2	25.01	0.15	0.72	0.19	1.50	30.01	0.24
W	0.2	0.5	0.3	25.01	0.15	0.72	0.18	1.46	30.01	0.27
X	0.3	0.2	0.5	25.01	0.15	0.72	0.18	1.46	30.01	0.27
Y	0.2	0.3	0.5	25.01	0.15	0.72	0.18	1.46	30.01	0.27

Step 3: In this step, the conflicts between the interacting Levels 1 and 2 are detected and managed through the designer's intervention. First, the loss in all three goals of Level 1 ($G_{J,Level\ 1}$, *where J = 1, 2, 3*) due to the choice of the solution for Level 2 is computed according to Equation 1. In the HRR problem, Level 'n' is Level 1, and Level 'n+1' is Level 2.

$$L\_G_{1,Level\ 1} = \frac{G_{1,Level\ 1_{satisficing}} - G_{1,Level\ 1_{achieved}}}{G_{1,Level\ 1_{satisficing}}} = \frac{290 - 279.81}{290} = 0.0351$$

Similarly $L\_G_{2,Level\ 1} = -0.0049$ and $L\_G_{3,\ Level\ 1} = -0.0736$.

Since all three goals are maximization goals, only positive loss values indicate conflict. Hence, conflict only exists for Goal 1, YS. The ARA module in the PDSIDES platform's PSA sub-template facilitates the above loss computation to detect conflicts. The designer checks for active design variables ($X_{K,Level\ 1}$) of Level 2 (total, m = 4) and active constraints to resolve this conflict. By comparing the $X_{K,Level\ 2}$ values in Table 4 with the variable bounds specified in the initial cDSP formulation of Level 2 – the KH of Level 2, the $X_{K,\ Level\ 2}$, d_γ (K = 1) is found to be near its lower variable bounds. Constraints on the lower limit of goal S_0 and the upper limit of goal d_α are found to be active. Hence, Approach 2 is chosen. The ARA module in the PSA sub-template of the PDSIDES platform facilitates the identification of active design variables and constraints.

The sensitivity of all three goals of Level 2 ($G_{J,Level\ 2}$, where J = 1, 2, 3), independently with respect to $X_{K,Level\ 2}$, d_γ, is computed using Equation 2. The sensitivity computations are performed for various combinations of all the remaining X_{n+1} values at either upper or lower bounds or nominal values. The above computation is illustrated here for the case of sensitivity of Goal 2 (d_α, J = 2) to the active design variable, d_γ. This requires the KH of Level 2 concerning the mathematical relations between $X_{Level\ 2}$ and $G_{J,Level\ 2}$ to be used. Hence, for C = 0.24%, Mn = 1.1%, and CR = 0.54 °C/s (all at their nominal values)

$$S_{2,X_{1,Level\ 2}} = \frac{G_{2,X_{UB,1,Level\ 2}} - G_{2,X_{LB,1,Level\ 2}}}{X_{UB,1,Level\ 2} - X_{LB,1,Level\ 2}} = \frac{33.11 - 24.00}{100 - 30} = 0.1303$$

The sensitivity values for different combinations of the remaining $X_{Level\ 2}$ are computed as above and are listed in Table 5 below. The largest value in magnitude from these calculated sensitivity values for Goal '2' is its sensitivity to $X_{1,Level\ 2}$ (d_γ). Hence, the sensitivity of Goal 2 (d_α) to d_γ, $S_{2,X_{1,Level\ 2}} = 0.1303$. Similarly,

the sensitivity of Goal 1 (X_f) to d_γ is $S_{1,X_{1,Level\,2}} = -0.00061$. The sensitivity of Goal 3 (S_0) to d_γ, is $S_{3,X_{1,Level\,2}} = 0$.

TABLE 5: Sensitivity values of d_α to d_γ for various combinations of other design variables

C (%)	Mn (%)	CR (°C/s)	$S_{2,X_{1,Level\,2}}$
0.24	1.1	0.1833	0.1303
0.24	1.1	0.9	0.1303
0.24	1.1	0.54	0.1303
0.18	1.1	0.54	0.1303
0.3	1.1	0.54	0.1303
0.24	0.7	0.54	0.1303
0.24	1.5	0.54	0.1303

The deviations of all 'J' goal values achieved at Level 2 compared to their targets are computed according to Equation 3, as given below.

$$D_{G_{1,\text{Level 2}}} = G_{1,\text{Level 2}\,target} - G_{1,\text{Level 2}\,achieved} = 0.882 - 0.725 = 0.158$$

Similarly, $D_{G_{2,\text{Level 2}}} = 8 - 25.01 = -17.01\ \mu m$ and $D_{G_{3,\text{Level 2}}} = 0.150 - 0.150 = 0\ \mu m$

Using the above goal deviations and the sensitivity values, the update required for design variable d_γ for a goal 'J' is computed using Equation 4. An example of the same is given below.

$$U_{2,X_{1,Level\,2}} = \frac{D_{G_{2,Level\,2}}}{S_{2,X_{1,Level\,2}}} = \frac{-17.01}{0.1303} = -130.544\ \mu m$$

TABLE 6: Design Variable update values for various goals and sensitivity values

J in $G_{J,Level\,2}$	$D_{G_{J,Level\,2}}$	$X_{K,Level\,2}$	$S_{J,X_{K,Level\,2}}$	$U_{J,X_{K,Level\,2}}$
1 (X_f)	0.158	d_γ (K=1)	-0.00061	-259.016
2 (d_α, µm)	-17.01	d_γ	0.1303	-130.544
3 (S_0, µm)	0	d_γ	0	0

The results of these computations are presented in Table 6. Only negative design variable update values are considered since the d_γ is at its lower bound. The largest value in magnitude in Table 6 is -259.016. This value is chosen to update the lower bound of d_γ. The above value is then used to compute the updated lower bound of the active design variable (d_γ) using Equation 5, as given below.

$$X_{1,\text{Level 2}\,Updated\ bound} = X_{1,\text{Level 2}\,Original\ bound} + U_{X_{1,\text{Level 2}}} = 30 - 259.016 = -229.016\ \mu m$$

The calculated updated bound for d_γ is practically infeasible. Thus, a practically feasible lower bound of 10 µm is selected based on values obtained from the literature [53]. Also, the constraint on the lower limit of Goal S_0 is relaxed to a smaller value of 0.10 µm, and the constraint on the upper limit of Goal X_f is relaxed to a larger value of 30 µm, based on the designer's domain knowledge. The design variable sensitivity computations and computation of updated active design variable bounds are facilitated by the ARA module in the PSA sub-template of the PDSIDES platform. The calculation of the updated limits of the active constraints can be facilitated by the CSA module in the PSA sub-template of the PDSIDES platform, which is not employed in this work.

TABLE 7: Information contained in the 'updated KHC' of Level 2

Sl. No.	Information
a.	Goal target values propagated from Level 1: $X_f = 0.883$, $d_\alpha = 8.000$ µm, $S_0 = 0.150$ µm.
b.	Microstructure-mechanical property models from cDSP of Level 1.
c.	Updated active design variable bounds: i) $X_{I,Level\ 2\ UB}$ (d_γ) = 10 µm.
d.	Updated active constraint limits: i) Lower limit on $S_0 = 0.10$ µm, and ii) Upper limit on $X_f = 30$ µm.

The updated variable bounds and relaxed constraint limit are propagated to the KHC of Level 2, summarized in Table 7. Level 2 cDSP is reformulated with these updated bounds and the relaxed constraint

limit as specified in Table A3 of Appendix A. Step 2 is repeated by executing the updated cDSP for different design scenarios. These scenarios and the satisficing solution space are visualized using ternary plots. The new satisficing solution space is defined by $d_\alpha \leq 15\mu m$, $S_0 \leq 0.125\mu m$, and $X_f \geq 0.7$. Using Figures 12a, 12b, and 12c, we represent the ternary plot for d_α, S_0, and X_f, respectively, corresponding to the updated Level 2 solutions. The superposed plot for Level 2 corresponding to the updated solutions is shown in Figure 12d. The yellow dashed line in Figures 12a and 11d, the orange dotted lines in Figures 12b and 12d, and the red chain line in Figures 12c and 12d represent the satisficing boundaries of d_α, S_0, and X_f, respectively, and the arrows indicate their feasible directions. The overall satisficing solution space of Level 2 corresponding to the updated solutions is highlighted in Figure 12d.

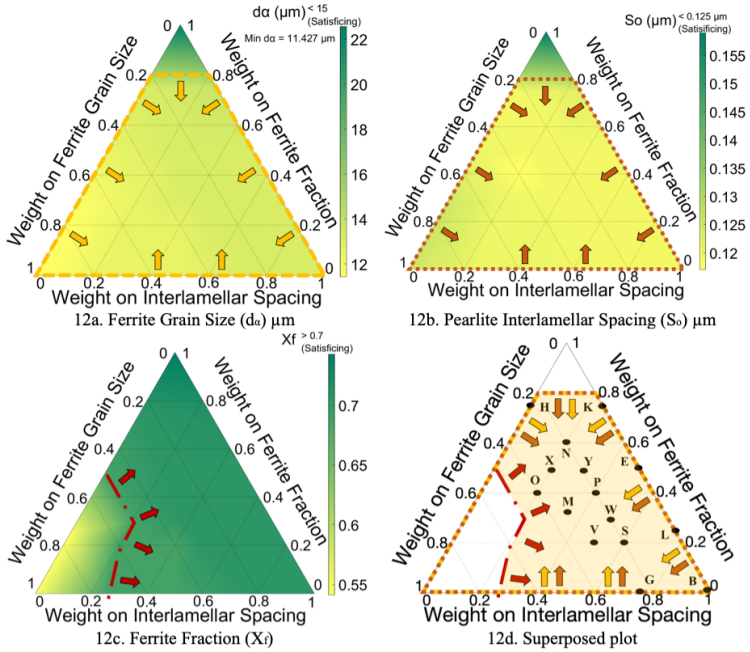

FIGURE 12: Ternary plots for goals d_α (12a), S_0 (12b), X_f (12c), and the superposed plot (12d) for Level 2 corresponding to the updated Level 2 solutions

The goal values corresponding to different design scenarios listed in Table 8 that fall in the satisficing space are mapped to the microstructure-mechanical property relations of Level 1 from the KHC of Level 2 to compute the corresponding Level 1 goal values. The designer's preference here is to pick a design scenario from Table 8 that yields the value closest to the satisficing targets (when the value is lower than the set satisficing targets) or exceeds the satisficing target by the greatest margin (when the value is larger than the set satisficing targets). In this case, the design scenario is selected by giving prime importance to the YS goal picked in Step 1 while still meeting the TS and HV goal requirements. Based on this criterion, the solution corresponding to design scenario O is chosen as the updated Level 2 solution. The selection is based on the computed values of Level 1 goals corresponding to the achieved Level 2 goal values and by looking into the designer's preference. The choice of design scenario O results in YS = 295.13 MPa, TS = 545.48 MPa, and HV = 140.72.

TABLE 8: Updated Level 2 solutions

Scenario	Weight on Goals (W_J)			Goals ($G_{J,n+1}$)			Design Variables (X_{n+1})			
	W_1	W_2	W_3	$G_{1,2}$ d_α (μm)	$G_{2,2}$ S_0 (μm)	$G_{3,2}$ X_f	C (%)	Mn (%)	d_γ (μm)	CR (°C/s)
B	0	1	0	13.100	0.119	0.707	0.18	1.50	10.04	0.79
E	0	0.5	0.5	13.100	0.119	0.707	0.18	1.50	10.04	0.79
G	0.25	0.75	0	13.094	0.119	0.707	0.18	1.50	10.02	0.79
H	0.25	0	0.75	13.089	0.119	0.707	0.18	1.50	10.00	0.79
K	0	0.25	0.75	13.761	0.122	0.714	0.18	1.50	10.00	0.68
L	0	0.75	0.25	13.100	0.119	0.707	0.18	1.50	10.04	0.79
M	0.33	0.34	0.33	13.100	0.119	0.707	0.18	1.50	10.04	0.79

N	0.2	0.2	0.6	13.100	0.119	0.707	0.18	1.50	10.04	0.79
O	0.4	0.2	0.4	12.543	0.117	0.701	0.18	1.50	10.00	0.90
P	0.2	0.4	0.4	13.100	0.119	0.707	0.18	1.50	10.04	0.79
S	0.2	0.6	0.2	13.100	0.119	0.707	0.18	1.50	10.04	0.79
V	0.3	0.5	0.2	13.094	0.119	0.707	0.18	1.50	10.02	0.79
W	0.2	0.5	0.3	13.100	0.119	0.707	0.18	1.50	10.04	0.79
X	0.3	0.2	0.5	13.100	0.119	0.707	0.18	1.50	10.04	0.79
Y	0.2	0.3	0.5	13.100	0.119	0.707	0.18	1.50	10.04	0.79

The updated solution and computed Level 1 goal values ($G_{J,Level\ 1}{}'$) corresponding to the updated Level 2 goal values are then propagated to the interaction space, and Step 3 is repeated to detect conflicts. The updated loss in all three goals of Level 1 ($L\_G_{1,Level\ 1}{}'$, where J = 1 to 3) due to the choice of the updated solution at Level 2, is recomputed according to Equation 1. This computation is carried out on the PDSIDES platform using the ARA module of the PSA sub-template.

$$L\_G_{1,Level\ 1}{}' = \frac{G_{1,Level\ 1\ satisficing} - G_{1,Level\ 1}{}'}{G_{1,Level\ 1\ satisficing}} = \frac{290 - 295.13}{290} = -0.0176$$

Similarly, $L\_G_{2,Level\ 1}{}' = -0.0909$ and $L\_G_{3,Level\ 1}{}' = -0.0824$

Since all three goals are maximization goals, only positive loss values indicate conflict. Hence, no conflicts are detected. As no further conflicts are not detected, the updated solution or decision at Level 2 is propagated inversely to the next level in the HRR system - Level 3, as its goals.

Using the information-decision framework, the designer can systematically identify and formulate the KH and KHC of Levels 1 and 2 and model the decision-making and interactions. Using the framework, the designer can detect conflicts between the decisions at the interacting levels regarding the YS goal of Level 1 not being satisfied by the initial set of solutions at Level 2. By using Approach 2, the designer is able to modify (expand) the design space at Level 2 and identify improved solution points that result in an improved value of YS by 13.32 MPa (approximately 4.6%) to 295.13 MPa. This brings all Level 1 goals to within satisficing limits. Using the information-decision framework, the designer is able to manage design conflict (MDC) between the interacting decisions at Levels 1 and 2 by realizing improved Level 2 solutions. With the improved Level 2 solutions, satisficing goal values for Level 1 are realized, thereby facilitating goal (FG) achievement and supporting the multilevel, top-down co-design of products, materials, and manufacturing processes. Using the HRR test problem, the capability offered by the information-decision framework to a designer in facilitating cooperative decision-making and supporting multilevel, top-down co-design in the design of products, materials, and manufacturing processes is demonstrated. The focus of the problem discussed is on the fulfillment of multiple conflicting product and process-related goals through the design of the material microstructure and processing paths in an inverse manner. PSPP relationships are used to model the problem as an integrated design of products, materials, and manufacturing processes. The proposed framework can be applied to support systematic information flow and cooperative decision-making across different levels to fulfill the end goals for complex problems characterized by the sequential information flow across models at different levels. The generic mathematical decision support constructs and the systematic information-decision workflow of the proposed framework facilitate this.

The proposed framework can also be utilized in a similar manner as discussed above to facilitate the co-design of the next set of interacting levels in the HRR system – Levels 2 and 3. For the next set of interacting levels, Level 2 will be considered Level ‘n,’ and Level 3 will be considered Level ‘n+1’ in the framework. The satisficing solution identified at Level 2 will become the goal target values at Level 3. The framework implementation will start with Step 2 by modeling the decision-making at Level 3 to achieve the goal targets propagated from Level 2. This is followed by Step 3 for conflict detection and management like the one demonstrated for Levels 1 and 2 interactions. By facilitating co-design between Levels 2 and 3 using the framework, designers can identify a satisficing set of rolling process parameters that meet the microstructure requirements propagated from Level 2. In this paper, we scope the use of the HRR test problem to demonstrate the framework's efficacy in supporting the co-design of products, materials, and manufacturing processes, which is realized by considering the interactions between Levels 1 and 2. The facilitation of the co-design between Levels 2 and 3 is beyond the scope of this paper and hence not presented.

5. CLOSING REMARKS

The realization of products or complex components that meet targeted performance requires the multilevel co-design of the product, materials, and manufacturing processes using PSPP relations. Design conflicts arise during the multilevel co-design of such systems when decisions made at one level with the constraints, bounds, and goals differ from the decisions of another interacting level. These design conflicts get propagated in a top-down manner for multilevel systems, adversely impacting the multilevel and system performance. Hence, there is a need to manage design conflicts by facilitating cooperation between decisions made across different levels. Enabling cooperation will help ensure improved multilevel and system performance and support multilevel co-design of products, materials, and manufacturing processes.

The information-decision framework presented in this paper allows the decision-maker to a) identify and formulate the Know-How (KH) and Know-How-to-Cooperate (KHC) of the interacting levels, b) model the decision-making of the interacting levels using the KH and KHC, c) detect conflicts between the interacting levels and d) manage conflicts by regulating decisions at the different levels using Approach 1 and Approach 2. To manage conflicts, Approach 1 uses a modification of design variable bounds, and Approach 2 combines Approach 1 with the modification of active constraint limits. The framework allows the designer to control the design space and decision-making of the interacting levels, facilitating cooperative decision-making during the top-down, multilevel co-design of systems involving products, materials, and manufacturing processes. The collaborative nature of multilevel decision-making using the framework helps realize improved multilevel and system performance by allowing the management of design conflicts and facilitating goal realization at the different levels. Based on the above contributions, the key functionalities offered to materials, product, and manufacturing process designers by the framework include:

- the capability to systematically detect and quantify the extent of conflicts between decisions at the interacting levels. Using the quantification of loss in goal values, the designer can establish priority between conflicts detected (in case of multiple conflicts) and choose the most important conflict to resolve;
- the capability to identify key active design variables (microstructure variables) and active constraints (process constraints), which, when appropriately modified (considering the practical feasibility of making changes), lead to reduced conflicts between multilevel decisions;
- a systematic approach using the proposed sensitivity metric to identify and manage key active design variables for achieving performance improvements or reducing conflicts. The approach, together with the metric, enables the designer to identify performance improvements possible with minimum resource utilization;
- a systematic approach to estimate the amount by which the key active variable bounds need to be changed to resolve design conflict. The estimate will serve as a guide for the designer to establish new bounds for active design variables for the next iteration;
- the capability to visualize the improvements in the solution spaces of the multilevel goals (using the ternary plots) between iterations. Using the visualization, the designer can make design choices among satisficing solutions more intuitively according to their preference, which is a benefit over other top-down design exploration approaches like IDEM;
- the capability to handle many design variables and goals (‘n’ number), which provides it an advantage in comparison with IDEM and other design exploration methods, which are limited by the number of goals and design variables that can be studied in multilevel systems design problems; and
- the capability to define new or updated requirements and goals at each level by formulating individual distributed but coupled cDSPs. This results in more flexible designs, leading to consistent system design where multilevel and system goals are physically feasible given the available resources— a benefit compared to IDEM and similar methods (which are based on mapping) and approaches that use an all-in-one formulation.

The framework is tested for the above functionalities using the HRR system design problem. Using the framework, the management of design conflicts between interacting Levels 1 and 2 is demonstrated. The design space regulation and decision-making are carried out using the framework by modifying design variable bound values and active constraints at Level 2, resulting in an improved Level 2 design space. The above improvement enables the designer to choose improved Level 2 solutions closer to target goals, resulting in a 4.6 percent improvement in the YS value (Level 1 goal), meeting the satisficing system goal targets. We also present the use of the template-based computational platform PDSIDES in formulating and

executing the cDSPs, exploring the solution space at multiple levels, and detecting and managing conflicts between interacting levels. The framework and related design constructs discussed are generic. The framework facilitates the top-down, sequential, multilevel co-design of systems involving products, materials, and manufacturing processes by promoting cooperative design decision-making to manage design conflicts. The top-down design of engineering systems characterized by sequential information flow can be accomplished using the framework presented.

ACKNOWLEDGMENTS

Anand Balu Nellippallil gratefully acknowledges support from NSF Award 2301808. The authors thank the support of the Department of Mechanical and Civil Engineering, Florida Institute of Technology. The authors thank Professors Janet K. Allen and Farrokh Mistree for their comments.

REFERENCES

1. Brockmöller, T., Siqueira, R., Gembarski, P. C., Mozgova, I., and Lachmayer, R., 2020, "Computer-Aided Engineering Environment for Designing Tailored Forming Components," *Metals*, vol. 10, no. 12, pp. 1589.
2. Laura, B., Vannila, P., Jens, K., Yusuf, F., M., Marius, L., Jörg, H., Malte, S., Thomas, H., Bernd, B., Bernd-Arno, B., Berend, D., Ludger, O., 2022, "Investigation of the Influence of the Forming Process and Finishing Processes on the Properties of the Surface and Subsurface of Hybrid Components," *The International Journal of Advanced Manufacturing Technology*, vol. 119, no. 1, pp. 119-136.
3. Aamer, N., Ozkan G., Kazi M., M., B., Onur E., Jingchao J., Jiayu S., Sajjad, H., 2023, "Multi-Material Additive Manufacturing: A Systematic Review of Design, Properties, Applications, Challenges, and 3D Printing of Materials and Cellular Metamaterials," *Materials & Design,* vol. 226, pp. 111661.
4. Nellippallil, A. B., Allen, J. K., Gautham, B. P., Singh, A. K., and Mistree, F., 2020, "Integrated Design of Materials, Products, and Associated Manufacturing Processes," Architecting Robust Co-Design of Materials, Products, and Manufacturing Processes, *Springer International Publishing*, *Cham*, pp. 1-45.
5. Arróyave, R., and McDowell, D. L., 2019, "Systems Approaches to Materials Design: Past, Present, and Future," *Annual Review of Materials Research,* vol. 49, no. 1, pp. 103-126.
6. Ashby, M. F., 1999, "Materials Selection in Mechanical Design," B*utterworth-Heinemann, Oxford.*
7. Pahl, G., Wallace, K., Blessing, L. T. M., Beitz, W., and Bauert, F., 2013, "Engineering Design: A Systematic Approach," *Springer, London*.
8. Shigley, J. E., 1972, "Mechanical Engineering Design," McGraw-Hill, New York, NY.
9. Olson, G. B., 2000, "Designing a New Material World," *Science*, vol. 288, no. 5468, pp. 993-998.
10. Pollock, T. M., Allison J. E., and co-authors, 2008, "Integrated Computational Materials Engineering: A Transformational Discipline for Improved Competitiveness and National Security", *The National Academies Press, Washington, DC*.
11. Olson, G. B., 1997, "Computational Design of Hierarchically Structured Materials," *Science*, vol. 277, no.5330, pp. 1237-1242.
12. McDowell, D. L., and Olson, G. B., 2009, "Concurrent Design of Hierarchical Materials and Structures," *Scientific Modeling and Simulations*, *Springer Netherlands, Dordrecht*, pp. 207-240.
13. McDowell, D. L., 2018, "Microstructure-Sensitive Computational Structure-Property Relations in Materials Design," *Computational Materials System Design*, *Springer International Publishing*, *Cham*, pp. 1-25.
14. Flores Ituarte, I., Panicker, S., Nagarajan, H. P. N., Coatanea, E., and Rosen, D. W., 2022, "Optimisation-Driven Design to Explore and Exploit the Process–Structure–Property–Performance Linkages in Digital Manufacturing," *Journal of Intelligent Manufacturing*.
15. Adams, B., Kalidindi, S., Fullwood, D. T., and Fullwood, D., 2012, "Microstructure Sensitive Design for Performance Optimization," *Elsevier Science*.
16. Kalidindi, S.-R., Niezgoda, S.-R., L, i., Giacomo, and Fast, T., 2010, "A Novel Framework for Building Materials Knowledge Systems," *Computers, Materials & Continua*, vol. 17, no. 2, pp. 103-126.
17. Kalidindi, S. R., Niezgoda, S. R., and Salem, A. A., 2011, "Microstructure informatics using higher-order statistics and efficient data-mining protocols," *JOM: The journal of the Minerals, Metals & Materials Society*, vol. 63, no. 4, pp. 34-41.
18. Chen, C. T., and Gu, G. X., 2020, "Generative Deep Neural Networks for Inverse Materials Design Using Backpropagation and Active Learning," *Advanced Science*, vol. 7, p. 1902607.
19. Kumar, S., Tan, S., Zheng, L., and Kochmann, D. M., 2020, "Inverse-Designed Spinodoid Metamaterials," *npj Computational Materials*, vol. 6, no. 1, p. 73.
20. Qian, C., Tan, R. K., and Ye, W., 2022, "Design of Architectured Composite Materials with an Efficient, Adaptive Artificial Neural Network-Based Generative Design Method," *Acta Materialia*, vol. 225, p. 117548.
21. Kim, B., Lee, S., and Kim, J., 2020, "Inverse Design of Porous Materials using Artificial Neural Networks," *Science Advances*, vol. 6, no. 1.

22. Tsai, K.-M., and Luo, H.-J., 2017, "An Inverse Model for Injection Molding of Optical Lens using Artificial Neural Network Coupled with Genetic Algorithm," J*ournal of Intelligent Manufacturing*, vol. 28, no. 2, pp. 473-487.
23. Kim, H. M., Michelena, N. F., Papalambros, P. Y., and Jiang, T., 2003, "Target Cascading in Optimal System Design," *Journal of Mechanical Design*, vol. 125, no. 3, pp. 474-480.
24. Kroo, I., Altus, S., Braun, R., Gage, P., and Sobieski, I., 1994, "Multidisciplinary Optimization Methods for Aircraft Preliminary Design," *Proceding of the 5th symposium on multidisciplinary analysis and optimization*, September 1994, Panama City Beach, FL, U.S.A, p. 4325.
25. Sobieszczanski-Sobieski, J., and Kodiyalam, S., 2001, "BLISS/S: A New Method for Two-Level Structural Optimization," *Structural and Multidisciplinary Optimization*, vol. 21, no. 1, pp. 1-13.
26. Sues, R. H., Oakley, D. R., and Rhodes, G. S., "Multidisciplinary Stochastic Optimization," *Proceedings of Engineering Mechanics*, ASCE, pp. 934-937.
27. Oakley, D. R., Sues, R. H., and Rhodes, G. S., 1998, "Performance Optimization of Multidisciplinary Mechanical Systems Subject to Uncertainties," *Probabilistic Engineering Mechanics*, vol 13, no. 1, pp. 15-26.
28. Du, X., and Chen, W., 2002, "Efficient Uncertainty Analysis Methods for Multidisciplinary Robust Design," *AIAA Journal,* vol. 40, no. 3, pp. 545-552.
29. Gu, X., Renaud, J. E., Batill, S. M., Brach, R. M., and Budhiraja, A. S., 2000, "Worst Case Propagated Uncertainty of Multidisciplinary Systems in Robust Design Optimization," *Structural and Multidisciplinary Optimization*, vol. 20, no. 3, pp. 190-213.
30. Shahan, D. W., and Seepersad, C. C., 2012, "Bayesian Network Classifiers for Set-Based Collaborative Design," *Journal of Mechanical Design*, vol. 134, no. 7, p. 071001.
31. Choi, H.-J., 2005, "A Robust Design Method for Model and Propagated Uncertainty," Ph.D Disseratatio, Georgia Institute of Technology.
32. Seepersad, C. C., Allen, J. K., McDowell, D. L., and Mistree, F., 2005, "Robust Design of Cellular Materials with Topological and Dimensional Imperfections," *Proceedings of the ASME 2005 International Design Engineering Technical Conferences and Computers and Information in Engineering Conference*, American Society of Mechanical Engineers, pp. 807-821.
33. Choi, H., McDowell, D. L., Allen, J. K., Rosen, D., and Mistree, F., 2008, "An Inductive Design Exploration Method for Robust Multiscale Materials Design," *Journal of Mechanical Design*, vol. 130, no. 3, pp. 031402.
34. Kern, P. C., Priddy, M. W., Ellis, B. D., and McDowell, D. L., 2017, "pyDEM: A Generalized Implementation of the Inductive Design Exploration Method," *Materials & Design*, vol. 134, pp. 293-300..
35. Nellippallil, A. B., Rangaraj, V., Gautham, B., Singh, A. K., Allen, J. K., and Mistree, F., 2018, "An Inverse, Decision-Based Design Method for Integrated Design Exploration of Materials, Products, and Manufacturing Processes," *Journal of Mechanical Design,* vol. 140, no. 11, p. 111403.
36. Wang, R., Nellippallil, A. B., Wang, G., Yan, Y., Allen, J. K., and Mistree, F., 2018, "Systematic Design Space Exploration using a Template-Based Ontological Method," *Advanced Engineering Informatics*, vol. 36, pp. 163-177.
37. Mistree, F., Smith, W., Bras, B., Allen, J., and Muster, D., 1990, "Decision-Based Design: A Contemporary Paradigm for Ship Design," *Transactions of the Society of Naval Architects and Marine Engineers*, vol. 98, pp. 565–597.
38. Simon, H.A., 1947, "Administrative Behavior," *Mcmillan, New York*.
39. Simon, H. A., 1956, "Rational Choice and the Structure of the Environment," *Psychological Review*, vol. 63, no. 2, pp. 129-138.
40. Mistree, F., Hughes, O., and Bras, B., 1993, "The Compromise Decision Support Problem and the Adaptive Linear Programming Algorithm," pp. 247-286.
41. Ming, Z., Nellippallil, A. B., Yan, Y., Wang, G., Goh, C. H., Allen, J. K., and Mistree, F., 2018, "PDSIDES-A Knowledge-Based Platform for Decision Support in the Design of Engineering Systems," *Journal of Computing and Information Science in Engineering*, vol.18, no. 4, pp. 041001.
42. Millot, P., & Lemoine, M. P., 1998, "An Attempt for Generic Concepts toward Human-Machine Cooperation", *Proceedings of IEEE International Conference on systems, man and cybernetics*, *San Diego, USA*, pp. 1044-1049.
43. Pacaux-Lemoine, M.-P., Trentesaux, D., Rey, G. Z., and Millot, P., 2017, "Designing Intelligent Manufacturing Systems through Human-Machine Cooperation Principles: A Human-Centered Approach," *Computers & Industrial Engineering*, vol. 111, p. 581-595.
44. Verhagen, W. J. C., Bermell-Garcia, P., Van Dijk, R. E. C., and Curran, R., 2012, "A Critical Review of Knowledge-Based Engineering: An Identification of Research Challenges," *Advanced Engineering Informatics*, vol. 26, no. 1, pp. 5–15.
45. Rocca, G. L., 2012, "Knowledge Based Engineering: Between AI and CAD. Review of a Language Based Technology to Support Engineering Design," *Advanced Engineering Informatics*, vol. 26, no. 2, pp. 159–179.
46. Ming, Z., Sharma, G., Allen, J. K., and Mistree, F., 2019, "Template-Based Configuration and Execution of Decision Workflows in Design of Complex Engineered Systems," Advanced Engineering Informatics, vol. 42, pp. 100985.
47. Reddy, R., Smith, W., Mistree, F., Bras, B., Chen, W., Malhotra, A., Badhrinath, K., Lautenschlager, U., Pakala, R., and Vadde, S., 1996, "DSIDES User Manual," Systems Realization Laboratory, Woodruff School of Mechanical Engineering, Georgia Institue of Technology, Atlanta, Georgia.

48. Hoc, J.-M., and Lemoine, M.-P., 1998, "Cognitive Evaluation of Human-Human and Human-Machine Cooperation Modes in Air Traffic Control," *The International Journal of Aviation Psychology*, vol. 8, no.1, pp. 1-32.
49. Trentesaux, D., and Millot, P., 2016, "A Human-Centred Design to Break the Myth of the "Magic Human" In Intelligent Manufacturing Systems," *Service orientation in holonic and multi-agent manufacturing, Springer*, pp. 103-113.
50. Pacaux, M.-P., Godin, S. D., Rajaonah, B., Anceaux, F., and Vanderhaegen, F., 2011, "Levels of Automation and Human-Machine Cooperation: Application to Human-Robot Interaction," *IFAC Proceedings Volumes*, vol. 44, no. 1, pp. 6484-6492.
51. Christopher Frey, H., and Patil, S. R., 2002, "Identification and Review of Sensitivity Analysis Methods," *Risk Analysis*, vol. 22, no. 3, pp. 553-578.
52. Morgan, M. G., Henrion, M., and Small, M., 1992, Uncertainty: A Guide to Dealing with Uncertainty in Quantitative Risk and Policy Analysis, *Cambridge University Press*.
53. P.,A., Manohar, Lim, K., AD, R., and Lee, Y., 2003, "Computational Exploration of Microstructural Evolution in a Medium C-Mn Steel and Applications to Rod Mill," *ISIJ international*, vol. 43, no.9, pp. 1421-1430.
54. Kuziak, R., Cheng, Y.-W., Glowacki, M., and Pietrzyk, M., 1997, "Modeling of the Microstructure and Mechanical Properties of Steels during Thermomechanical Processing," *NIST Technical Note(USA)*, vol. 1393, p. 72.
55. Yada, H., 1988, "Prediction of Microstructural Changes and Mechanical Properties in Hot Strip Rolling," *Proceedings of the Metallurgical Society of the Canadian Institute of Mining and Metallurgy*, *Elsevier*, pp. 105-119.
56. P., D., Hodgson, 1992, "A Mathematical Model to Predict the Mechanical Properties of Hot Rolled C-Mn and Microalloyed Steels," *ISIJ international*, vol. 32, no.12, pp. 1329-1338.

APPENDIX A

In Table A1, the models that relate the steel microstructure and composition design variables after the cooling process with the mechanical property goals are presented. These models are used at Level 1 in the HRR problem; see Step 1 in Section 4.

TABLE A1: Empirical models for mechanical properties at Level 1

(T_{mf} = 700 ^{0}C, p = 6 μm, t_{carb} = 0.025 μm)

Mechanical Property	Empirical Model	Source
YS	$X_f(77.7+59.9[Mn]+9.1(d_\alpha*0.001)^{-0.5}) + 478[N]^{0.5} + 1200[P] + (1-X_f)(145.5+3.5S_0^{-0.5})$	Kuziac et.al. (1997) [54]
TS	$X_f(20+2440[N]^{0.5} + 18.5(0.001*d_\alpha)^{-0.5} + 750(1-X_f) + 3(1-X_f^{0.5})S_0^{-0.5} + 92.5*[Si]$	Kuziac et.al. (1997) [54]
HV	$X_f(361-0.357T_{mf}+50[Si]) + 175(1-X_f)$	Yada (1987) [55]

In Table A2, the models that relate the cooling process parameters with the steel microstructure after the cooling process are presented. These models are used at Level 2 in the HRR problem; see Step 2 in Section 4.

TABLE A2: Empirical models for microstructure characteristics at the end of the cooling process at Level 2

Microstructure characteristics	Empirical Models	Source
d_α	$(1-0.45\varepsilon_r^{0.5})*\{(-0.4 + 6.37*C_{eq}) + (24.2 - 59*C_{eq})CR^{-0.5} + 22*(1-\exp(-0.015*d_\gamma))\}$	Hodgson & Gibbs (1992) [56]
S_0	$0.1307+1.027[C]-1.993[C]^2 - 0.1108[Mn]+0.0305*CR^{-0.52}$	Kuziac et.al. (1997) [54]
$X_{f\,eq}$	$1 - ([C]/(0.789-0.1671[Mn]+(0.1607[Mn]^2) - (0.0448[Mn]^3)))$	Kuziac et.al. (1997) [54]
X_f	$X_{f\,eq} - 5.48(1-\exp(-0.0106CR)) - (0.723*(1-\exp(-0.0009d_\gamma)))$	Kuziac et.al. (1997) [54]
C_{eq}	([C] + [Mn])/6	Hodgson & Gibbs (1992) [56]

In Table A3, the cDSP formulations for Levels 1 and 2 of the HRR problem are presented. The cDSPs are discussed in Section 4, Steps 1 and 2. In Table A3, the values in bold font and the '*' symbol adjacent to it indicate locations where changes are made to the initial cDSP formulation at Level 2. The changes made to the cDSP are discussed in Section 4, Step 3. These changes are listed below in bold font, along with the '#' symbol adjacent to it.

Level constraints i, ii, and v for Level 2

i. $8 \leq d_\alpha \leq \mathbf{30}^{\#}$ (μm)

ii. **0.10** $^{\#} \leq S_0 \leq 0.25$ (μm)
v. **10** $^{\#} \leq d_\gamma \leq 100$

Variable bound iii for Level 2
iii. **10** $^{\#} \leq X_9 \leq 100$ (μm)

TABLE A3: cDSP formulations of interacting Levels 1 and 2 in the HRR system

Level 1	Level 2
GIVEN	
a. End requirements of Level 1 in terms of Mechanical properties required i. Goal G_1: Maximize YS [MPa] ii. Goal G_2: Maximize TS [MPa] iii. Goal G_3: Maximize HV	a. End requirements of Level 2 in terms of microstructure characteristics at the end of cooling process i. Maximize X_f ii. Minimize d_α iii. Minimize S_0
b. Well-established mathematical models for these properties in terms of the design variables, see Table A1 above	b. Well established mathematical models for the above requirements in terms of the design variables, see Table A2 above
c. Design variables (X_p) and their bounds: X_1: Ferrite fraction, X_f X_2: Ferrite grain size, d_α (μm) X_3: Pearlite interlamellar spacing, S_0 (μm) X_4: Silicon concentration, [Si] (%) X_5: Nitrogen concentration, [N] (%) X_6: Manganese concentration after cooling process, [Mn] (%)	c. Design variables (X_P) and their bounds X_7: Carbon concentration, [C] (%) X_8: Manganese concentration after rolling, [Mn] (%) X_9: Austenite grain size, d_γ X_{10}: Cooling rate, CR (°C/s)
FIND values of	
a. Design variables: X_P (for P = 1,2,3,4,5,6)	a. Design variables: X_P (for P = 7,8,9,10)
b. Deviation variables: d_1, d_2, and d_3	b. Deviation variables: d_4, d_5, and d_6
SATISFY	
a. Level constraints i. $220 \leq YS \leq 330$ (MPa) ii. $450 \leq TS \leq 750$ (MPa) iii. $131 \leq HV \leq 170$	a. Level constraints i. $8 \leq d_\alpha \leq$ **25 *** (μm) ii. **0.15 *** $\leq S_0 \leq 0.25$ (μm) iii. $0.5 \leq X_f \leq 0.9$ iv. $C_{eq} < 0.35$ v. **30 *** $\leq d_\gamma \leq 100$ vi. $0.1833 \leq CR \leq 0.9$
b. Level goals: i. $\{YS(X_p)/YS_{target}\} + d_1^- - d_1^+ = 1$ ii. $\{TS(X_p)/TS_{target}\} + d_2^- - d_2^+ = 1$ iii. $\{HV(X_p)/HV_{target}\} + d_3^- - d_3^+ = 1$	b. Level goals: i. $\{d_{\alpha\ target}/d_\alpha(X_P)\} + d_4^+ - d_4^- = 1$ ii. $\{S_{0\ target}/S_0(X_P)\} + d_5^+ - d_5^- = 1$ iii. $\{X_f(X_P)/X_{f\ target}\} + d_6^- - d_6^+ = 1$
c. Variable bounds i. $0.1 \leq X_1 \leq 0.9$ ii. $8 \leq X_2 \leq 25$ (μm) iii. $0.15 \leq X_3 \leq 0.25$ (μm) iv. $0.18 \leq X_4 \leq 0.3$ (%) v. $0.007 \leq X_5 \leq 0.009$ (%) vi. $0.7 \leq X_6 \leq 1.5$ (%)	c. Variable bounds i. $0.18 \leq X_7 \leq 0.30$ (%) ii. $0.7 \leq X_8 \leq 1.5$ (%) iii. **30 *** $\leq X_9 \leq 100$ (μm) iv. $0.1833 \leq X_{10} \leq 0.9$ (°C/s)
d. Deviation variable bounds $d_i^+, d_i^- \geq 0$ and $d_i^+ * d_i^- = 0$	d. Deviation variable bounds $d_i^+, d_i^- \geq 0$ and $d_i^+ * d_i^1 = 0$

MINIMIZE	
The deviation function (Z_1). Min $Z_1 = \boldsymbol{\Sigma}\ W_i\,(d_i^+ + d_i^-)$, where, W_i = weights assigned to the deviations of the individual goals from the target values, $\boldsymbol{\Sigma}\ W_i$ = 1, and i = 1, 2, 3.	The deviation function (Z_2). Min $Z_2 = \boldsymbol{\Sigma}\ W_i\,(d_i^+ + d_i^-)$, where, W_i = weights assigned to the deviations of the individual goals from the target values, $\boldsymbol{\Sigma}\ W_i$ = 1 and i = 4, 5, 6